



Republic of Iraq
Ministry of Higher Education
and Scientific Research
University of Kerbala
College of Education for Pure Sciences
Department of Chemistry

***Comparison among three solutions
for production of porous silicon***

A thesis

The Council of Education for pure Sciences-University of
Kerbala In partial Fulfillment of the Requirements for the
Master Degree in Chemistry.

By :

Furqan Saleh Mahdi
(B.Sc.2019)

Supervisor By :

Prof. Dr.Hamida Idan Salman

Assist Prof .Dr.Ahmed.K.Al-Kadumi

1444 A.H

2022 A.D

بِسْمِ اللَّهِ الرَّحْمَنِ الرَّحِيمِ

(وَإِذْ آتَيْنَا مُوسَى الْكِتَابَ وَالْفُرْقَانَ لَعَلَّكُمْ تَهْتَدُونَ)

صدق الله العلي العظيم

البقرة (53)

Supervisor's Certificate

I certify that this thesis entitled " Comparison among three solutions for production of porous silicon " was prepared by (Furqan Saleh Mahdi) under my supervision at the College of Education for Pure Sciences _ University of Karbala in a partial fulfillment of the requirements for the master of Science Degree in Chemistry .

Signature:



Prof. Dr. Hamida Idan Salman

Date: 16/1/2023

Signature:



Asst. Prof. Dr. Ahmed.K.Al-Kadumi

Date: 16/1/2023

In view of the available recommendations, I forward this thesis for debate by the examining committee.

Signature:

Name: Dr. Sajid Hassan Guzar

Sci. Title: Assistant Professor

Date: 16/1/2023

Head of Department of Chemistry

Amendment Report

This is to certify that the thesis entitled (Comparison among three solutions for production of porous silicon) and has been corrected and the researcher has been completed all the grammatical mistakes . Therefore, I Confirm that current thesis is qualified for debate.

Signature:

Name: *Shaymaa Abid Abdulameer*

Sci. title: Instructor *Doctor*

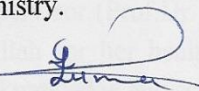
Address: University of Karbala

Date: *12/1/2023*

Committee Certificate

We certify that we have read this thesis entitled "Comparison among three solutions for production of porous silicon" and, as an examining committee, examined the student (Furqan Saleh Mahdi) in its content and that in our opinion; it is adequate with standing as a thesis for the of Master of Science Degree in Chemistry.

Chairman

Signature: 

Name: Dr. Luma Majeed Ahmed

Sci. Title prof.

Address: University of Kerbala

Date: 15. 1. 2023

Member

Signature: 

Name: Khawla Kinee Jasim

Title Assist. Prof

Address: University of AL-Muthanna

Date: 16/1/2023

Member

Signature: 


Name: Muhammad Al-Baghdadi

Title: professor

Address: University of Kerbala

Date: 15/1/2023

Supervisor & Member

Signature: 


Name: Dr. Hamida Idan Salman

Title: Professor

Address: University of Kerbala

Date: 16/1/2023

supervisor & member

Signature: 

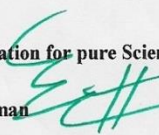
Name: Dr. Ahmed .K.AL-kadumi

Title: Assi prof

Address: University of Kerbala

Date: 15/1/2023

Approved by the Collage of Education for pure Sciences, University of Kerbala .

Signature: 

Name: Prof .Dr.Hamida Idan Salman

Date: 18/1/2023

Acknowledgments

Praise be to Allah, the best grader, I thank Him and thank Him in recognition of the grace that he opened to me from the vast and generous virtues, and prayers and peace be upon the most honorable Prophet Muhammad (May Allah prayers be upon him and upon his pure household).

I am so honored to thank my supervisor (Prof.Dr. Hamida idan salman) for her support, We pray to Allah for her health and safety and she continue serving as a beacom for knowledge and science.

I am also honored to extend my sincere thanks and gratitude to my supervisor (Dr. Ahmed Kherallah Al-kadumi),for his morals and support in every possible way, and the distinguished and continuous efforts he showed to accomplish this work.

Finally, I extend my thanks and gratitude to everyone who called for good and facilitation to help me complete this work .

Furqan

Dedication

to Allah whom mentioned is contentment and success . And to those who are not disappointed by the hope who supported me in every adversity and gave me their strength and patience and chose the right path for me (the pure imams).

To the one who gave me life and gave me life to the one who are bringing me up in the faith and love of the most merciful to those who stood by me until I advanced to success (my dear father & my mother).

To the one lasting support, my dear husband.

I want to express my gratitude and devotion to everyone who helped me complete this project.

FURQAN

Abstract

Porous silicon has been studied by its physical, chemical and structural properties

The results of the used acids were studied (HF + HNO₃ , HNO₃ + Salt (NaCl) and HF + Ethanol) and compared by studying the morphological and structural properties of the porous silicon layers using scanning electron microscopy (SEM), X-ray diffraction (XRD) and gravimetric method.

Through the electron microscope images, it was found that there are different shapes, as the shape varies according to the time of the interaction

Pore width and thickness of porous silicon layer increase using nitric acid with HF more than using HF with ethanol.

The measured porosity by using gravimetric methods varies according to the acids used to produce porous silicon, it appeared with higher values in nitric acid than using ethanol with HF.

The optical and electrical properties of citrus samples were studied and it was found that these properties are affected by the thickness of the layer.

The electrical capacitance is affected by the porosity and the thickness of the layer, if it decreases, the larger the porous layer is due to the amount of charges and ions present, but when the porous layer becomes small, it decreases due to the presence of air.

The electrical capacitance of silicon nanoparticles produced by HF with ethanol is much higher than that of HNO₃ with HF.

The difference in the measurement of the nanoscale dimensions of the pores during different times of HF + Ethanol acid is more uniform and its nano properties are clearer because the smaller the pores, the clearer the nanoscale characteristics.

Silicon reacts with nitric acid to produce the oxide that dissolves in hydrofluoric acid. Thus, the reaction with nitric acid in the presence of HF gave the best and finest porous silicon.

In general, the properties of porous silicon production from the reaction for silicon with acids this causes to make optimization for this porous characteristics in the light of the any application of nano crystalline silicon.

List of Content

Contents	Page
Table of Content	I
List of Tables	III
List of Figures	III
List of Symbols and Abbreviations	VI
Chapter One: Introduction	
1-1 Introduction	1
1.2 Silicon Element	5
1.3 Porous Silicon	6
1.4 Methods for Producing Porous Silicon	7
1.4.1 Dry Etching	8
1.4.2 Wet Etching	8
1.4.2.1 Electrochemical Etching	9
1.4.2.2 Stain Etching Technique	11
1.4.2.3 Electrophotochemical Etching	11
1.4.2.4 Etching done with photochemicals	12
1.5 Porous Silicon's Unique Characteristics	12
1.5.1 The Chemical Characteristics	13
1.5.2 The Physical Characteristics	13
1.5.3 Porous Silicon Structure	14
1.5.3.1 The X-ray Diffraction	14
1.5.3.2 morphological Features	15
1.5.3.2 a. pore Type	15
1.5.3.2 b. pore Size	16
1.5.3.2 c. pore Form	17
1.5.3.2 d. The Porosity	18
1.5.3.2. e. The Surface area	18
1.5.4. Optical Characteristics	19
1.5.5 Electrical capacitance of a silicon layer with pores	21
1.6. Extensive Use of Porous Silicon	22
1.7 Hydrogen Fluoride	23
1.8 Historical Review	24
Aims of Study	27

Chapter Two: Experimental part	
2.1 Introduction	28
2.2 The Materials and Equipment Utilized in this Research	28
2.3 Preparation of Samples	29
2-4 The Measurements	32
2-4-1 Gravimetric Measurements	32
2-4-2 Optical Measurements	34
2-4-3 Rate of Etching Measurements	34
2.4.4 Measurement of Porous Silicon's Electrical Capacitance	34
2.4.5 The X-Ray Diffraction Technique	35
2.4.6 The Scanning Electron Microscope (SEM)	35
Chapter Three: Results and Discussion	
3.1 Introduction	36
3.2 Structure properties in a layer of porous silicon	36
3.2.a The porosity	36
3.2.b Layer Thickness	39
3.2.c Scanning Electron Microscope (SEM)	42
3.3 Optical Properties	47
3.3.a. Relative Permittivity and Refractive index	48
3.4 The Electrical Capacitance for Ps Layer	51
3.5 Porous silicon's X-Ray Characteristics	53
Chapter Four: Conclusions and Recommendations	
4.1 Conclusions	57
4.2 Recommendations	59
References	
	60

List of Tables

No.	Title	Page
(1.1)	IUPAC Classifies pores based on size.	17
(1-2)	Application of porous silicon.	22
(2.1)	The Equipment Utilized in the Research	28
(2.2)	The Materials used	29
(3-1)	Pore size for Samples.	47

List of Figures

No.	Title	Page
(1-1)	Direct and indirect semiconductor band gap.	6
(1-2)	The Typical Distribution of Ps Components, Shown in a Schematic.	7
(1-3)	Schematic of the interface between Porous Silicon and bulk silicon.	10
(1-4)	Bulk Si and Porous silicon X-Ray Diffraction.	15
(1-5)	Types of pores: (a, b) Blind, Dead end. (c) Interconnected or Branched. (d) Totally isolated or Closed and (e) Through pores.	16
(1-6)	Pore shapes: (a) cylindrical (b) Ink-bottle (c) Funnel (d) Cuboid or slit and (e) Triangular or Pyramidal.	18
(1-7)	Absorption spectra of crystalline silicon and (Ps)	20
(1-8)	Capacitance of Ps layers (a) porosity & (b) layer thickness.	21
(1-9)	Hybridization of HF.	24
(2-1)	Wafer photo (a) prior to cutting the bulk silicon (b) After a silicon-cutting.	30

(2-2)	The systematic for electrochemical etching which used in this study.	31
(2-3)	A picture of an ethanol sample.	32
(2-4)	Photograph when porous layer was removing in KOH.	33
(3-1)	Relation between porosity and Etching time for Nitric acid and HF	37
(3-2)	Relation between porosity and Etching time for Ethanol and HF.	38
(3-3)	Relation between the and porosity etching time for both solutions.	38
(3-4)	Relationship between layer thickness and Etching time with Ethanol and HF.	40
(3-5)	Relationship between layer thickness and Etching time with Nitric acid and HF.	41
(3-6)	Relationship between layer thickness and Etching time for both solutions.	41
(3-7)	SEM image of Ps layer with HNO ₃ +HF at 5 min.	42
(3-8)	SEM image of Ps layer with HNO ₃ +HF at 25 min.	43
(3-9)	SEM of Ps layer in HF+ Ethanol at 5 min	44
(3-10)	SEM of Ps layer in HF + Ethanol at 15 min.	44
(3-11)	SEM of Ps layer in HF + Ethanol at 25 min.	45
(3-12)	SEM of Ps layer in Nitric acid + salt at 15 min.	46
(3-13)	SEM of Ps layer in Nitric acid + salt at 20 min.	46
(3-14)	Relation between Refractive index and time for Nitric acid and HF.	49
(3-15)	Relation between Refractive index and time for Ethanol and HF.	49
(4-16)	Relation between Refractive index and time for both solutions.	49
(3-17)	Relation between Relative permittivity and time for Nitric acid and HF.	50
(3-18)	Relation between Relative permittivity and time	51

	for Ethanol and HF.	
(3-19)	Relation between Relative permittivity and time for both solutions.	51
(3-20)	Relation between capacitance and Etching time of Nitric acid +HF.	52
(3-21)	Relation between capacitance and Etching time of Ethanol + HF.	52
(3-22)	Relation between capacitance and Etching time of both solutions.	53
(3-23)	X-Ray Diffraction of Ps in HNO ₃ +SALT at 15 min.	54
(3-24)	Figure X-Ray Diffraction of Ps in HNO ₃ +SALT at 20 min.	54
(3-25)	Figure X-Ray Diffraction of Ps in HF+ Ethanol at 15 min.	55
(3-26)	X-Ray Diffraction of Ps in HF + Ethanol at 20 min.	55
(3-27)	X-Ray Diffraction of HNO ₃ +HF at 5 min.	56
(3-28)	X-Ray Diffraction of HNO ₃ +HF at 25 min.	56

List of Symbols and Abbreviations

Symbol and Abbreviation	Meaning	Unit
D	Layer thickness of Porous silicon	Cm
E _g	Energy gap of silicon wafer	eV
C _{psi}	Capacitance of Psi layer	Farad
K	Boltzmann s constant	J / K
Hv	Photon energy	eV
m ₁	Weight of silicon sample before etching process	g
m ₂	Weight of silicon sample after etching rate	g
m ₃	Weight of silicon sample after removing porous silicon layer	g
A	The area of the freckled surface	Cm ²
T	Etching time	Minute
V	Etching rate	Cm/ min
ε _{pore}	Relative Permittivity of air	-
ε _{si}	Relative Permittivity of silicon	-
ε ₀	Relative Permittivity of free space	F/cm
ε _{psi}	Relative Permittivity of porous silicon	-
EC	Electro chemical	-
HF	Hydrofluoric	-
HNO ₃	Nitric acid	-
Ps	Porous silicon	-
FTIR	Fourier transform infrared spectroscopy	-
SEM	Scanning electron micr oscopy	-
HRSEM	High resolution scanning electron microscopy	-
HRTEM	High resolution transmission electron microscopy	-
SPF	Surface porous film	-
XRD	X- Ray diffraction	-

Chapter One

Introduction

1.1. Introduction

Nanotechnology uses atomic, molecular, and supramolecular materials in industry. National Nanotechnology Initiative described nanotechnology as manipulating matter with 1 to 100 nanometer dimensions. Nanotechnology, is defined by size, includes surface science, organic chemistry, molecular biology, semiconductor physics, energy storage, engineering, microfabrication, and molecular engineering [1].

Nanotechnology can generate novel materials and gadgets for nanomedicine, nanoelectronics, biomaterials, energy production, and consumer items. Nanotechnology engineers atomic-scale materials. Classical physics and chemistry don't work well at this scale for two reasons. First, small molecules' electrical characteristics can be substantially different from bigger ones. Second, since surface atoms are the most reactive, the material's characteristics alter unexpectedly. Nanoparticles have attracted more researchers in the previous decade. Nanoparticles' small size, which affects their electrical, optical, magnetic, chemical, and mechanical properties, making them suited for modern applications [2] [3].

Nanotechnology will impact every industry by improving existing products and materials, creating new materials, and advancing electronics, energy, and healthcare [4].

Nanoscience studies ultra-small structures and materials and their unique features. Scientists from chemistry, physics, biology, medicine, computing, materials science, and engineering research nanoscience to better comprehend our world. Nanotechnology designs, produces, and applies nanoscale structures, devices, and systems. One studies

nanomaterials and their qualities, while the other uses them to create something new[5].

Silicon's potential role in optoelectronics has been the subject of numerous studies and reports published in the years following the year 1990 [6].

Silicon is the most important component in today's microelectronics. The high qualities and processing features, in addition to the huge body of supporting technology that has grown up around it, are directly responsible for its superiority over all other semiconductors. This dominance is also tightly related to the tremendous base of technology that has developed around it. It is highly unlikely that silicon will be supplanted as the go-to material for electronic applications by any other semiconductors [7].

Silicon, on the other hand, a light emitter that is extraordinarily inefficient, and this is the primary reason why it has not enjoyed the same level of dominance in optical applications [8].

Electro-chemical etching is capable of producing porous silicon (Ps) based on experimental data. In contrast to the more complicated procedures necessary for solid-state processing, the capacity to produce junctions is utilized in electronic testing in less complex ways.

The spot etching process of silicon wafers (also known as chemical etching) is one of the most popular techniques. This technology can be used to prepare porous silicon, which then possesses optical and electrical properties that make it suitable in a wide variety of optoelectronic devices, such as photodetectors, solar cells, and display devices [9].

In the past two decades, Ps has developed into a material that is widely used by scientists and technologists, and it has been put to use in a variety of different fields [10].

A network of voids can be found throughout the mass of porous silicon, which can be thought of in the same way as crystalline silicon. A structure made of nanocrystals that looks like a sponge with holes and channels. is produced as a result of the voids in the silicon block. This technology will have very significant repercussions not only economically, but also socially and environmentally. A microporous material (Ps) that PL in the visible region of the electromagnetic spectrum can be produced by certain electrochemical etching processes applied to silicon, as was demonstrated in recent research. Due to the one-of-a-kind role that silicon plays in contemporary electronic technology, the remarkable luminescence of this material has attracted a lot of attention [11].

A-dvanced manufacturing technology, porous silicon is rapidly becoming a material for electronic components that is in high demand and offers a wide range of applications [12].

Ps has been primarily obtained by oxidation in an aqueous or ethanoic solution of HF ever since the early studies of Turner and Uhlir and later by Canham. This method has been used [13].

Porous silicon is a particularly promising material due to its excellent thermal and mechanical characteristics, apparent compatibility with silicon-based microelectronics, inexpensive cost, its ability to vary the refractive index with respect to depth, controllable pore sizes, convenient surface chemistry, and large surface area within a small volume, porous silicon is an ideal insulating material for the formation of

multiple layers. All of these characteristics, taken together, give rise, on the one hand, to an interest in the optical properties that can be achieved by combining silicon and air using an effective mean approximation [14] [15].

On the other hand, pores permit the penetration of chemical, biological, and liquid cell molecules, which can change the optical behavior of the native system. This can be useful in a variety of applications. These factors sparked interest in research into a variety of applications including , applications in optical sensing and biomedicine both need to be considered [16].

Porous silicon light-emitting devices have been developed in recent years, expanding the scope of possible optoelectronics applications. Although there is still much work to be done to increase their dependability, research on optical interfaces has shown that electroluminescent porous silicon devices perform better when paired with photodetectors. The realization of a full Silicon-based photoelectronic system relies heavily on porous silicon, the crystalline structure of silicon and the nature of its bonds are discussed, as the quantum confinement design and the technical steps involved in making porous silicon, the characterization of the physical and chemical properties is essential to a wide range of useful uses [17].

1.2. Silicon Element

Silicon is a chemical element in the carbon family that is not a metal. (group IV of the periodic table). It comprises 27.7 percent of the Earth's crust, making it the second most abundant crustal component. Owing to its high surface oxygen absorption and oxide layer development rate, silicon is a common material for semiconductors [18].

Crystalline silicon (c-Si), the backbone of the current electronics industry, is an indirect semiconductor with a band gap about 1.12eV at ambient temperature and can only emit feeble light in the near infrared without external power. Since compound semiconductors like GaAs, InP, etc. have narrower band gaps, they are currently the preferred material for use in optoelectronics, limiting the usefulness of silicon in this field. The challenges in integrating these chemicals with mature Si, integrated technology impede their widespread use and continued development. However, this trend has recently been reversed due to the discovery of strong visible photo-luminescence and electroluminescence in porous silicon and similar materials [19] [20]. .

The photoluminescence period is measured in seconds because the probability of a three-particle reaction is so low. It is clear from Figure (1-1) that bulk crystalline Si is an extremely inefficient optical and electrical excitation light generating medium.

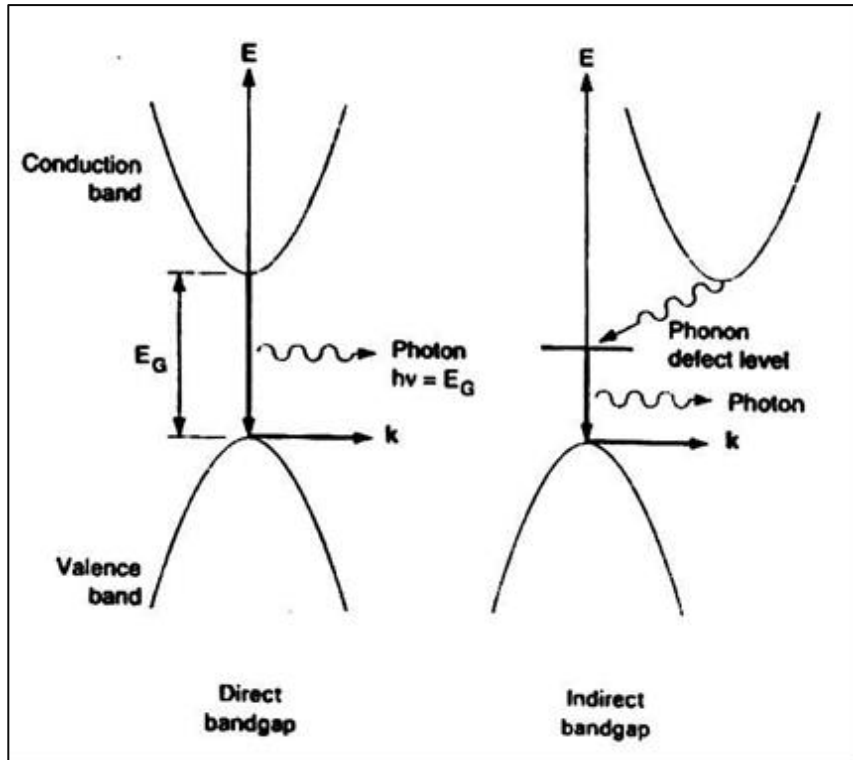


Figure (1-1) Direct and indirect semiconductor band gap [21].

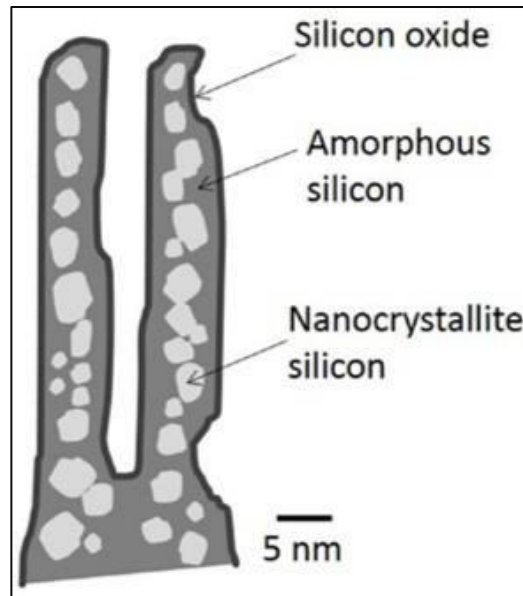
1.3. Porous Silicon

Porous silicon has a network of holes in it. that are separated from one another by thin walls and has nano-crystalline silicon included into the surface morphology [22].

In 1956, Uhlir was the first person who detected that porous silicon was produced on the top of substrates made of crystalline silicon when exposed to hydrofluoric acid (HF) at the right anodic inclination. In this paper the electro polishing was investigated and made the discovery under a given threshold of current density, A brownish layer developed [23].

Today, this film is called "porous silicon." and it was his discovery. Turner continued his research on porous silicon and investigated it in greater depth because At the time, it was a bother. By using the method of

etching, raw crystalline silicon is converted to the form of a sponge consisting of intertwined With pores and channels in silicon coated with hydrogen [24], as is illustrated diagrammatically in the Fig (1-2).



Figure(1-2) The Typical Distribution of Ps Components [25].

Conditions pertaining to doping and etching have a significant impact on both the size of the pores and the silicon skeleton that is left behind [26] .

Porous silicon has a high surface area to volume ratio, in addition to the quick oxidation rate that is associated with it, has captured the attention of researchers for a significant amount of time [27].

1.4. Methods for Producing Porous Silicon

There are four methods to approaches the fabricating (Ps) layers are etching procedures (stain, photochemical, electrochemical, and photo electrochemical) Etching, The properties of the shaped (Ps) layer produced by each of these processes are distinct from one another [28]. There is a preponderance of subtractive technique of structure formation

in micro technology. Etching technique's significance is thus revealed. In etching processes, the useful material is removed locally, typically through the openings of a resist mask. Whether the removed substance is transformed into a liquid or a gas defines the distinction between wet and dry etching processes. In order to remove material from the surface of a solid-state substrate, all etching processes must first convert the removed material into a mobile state. And the transfer into the gas phase calls for rapidly evaporable compounds of the effect of strong impulses to remove atoms or clusters from the substrate, while the liquid phase calls for soluble species. It is common practice to classify Etching into two broad categories [29].

1.4.1. Dry Etching

Based on chemical processes that take place at the boundary between gas and solid. Etching semiconductor plates in a gas environment requires the employment of rapid laser pulses with high power densities, which can be generated by excitation energy or CW (Continuous - wave) visible laser. When compared to stain etching, When compared to wet etching, the pace and thickness of porous silicon growth produced by dry etching are dramatically greater [30].

1.4.2. Wet Etching

The chemical etching process takes place at the interface between the liquid and the solid. Two approaches differ in a number of significant ways, Most notable of which are the rate of growth and the thickness of the porous coating. A new method for the formation of porous semiconductors has been proposed by Kalem and Yavuzcetin [31]. This method depends on letting the surface of the semiconductor to etchants that work in the gas phase that demonstrate luminescence at

approximately 750 nm. Wet etching utilizes a variety of techniques, each of which produces porous silicon in a different way [32].

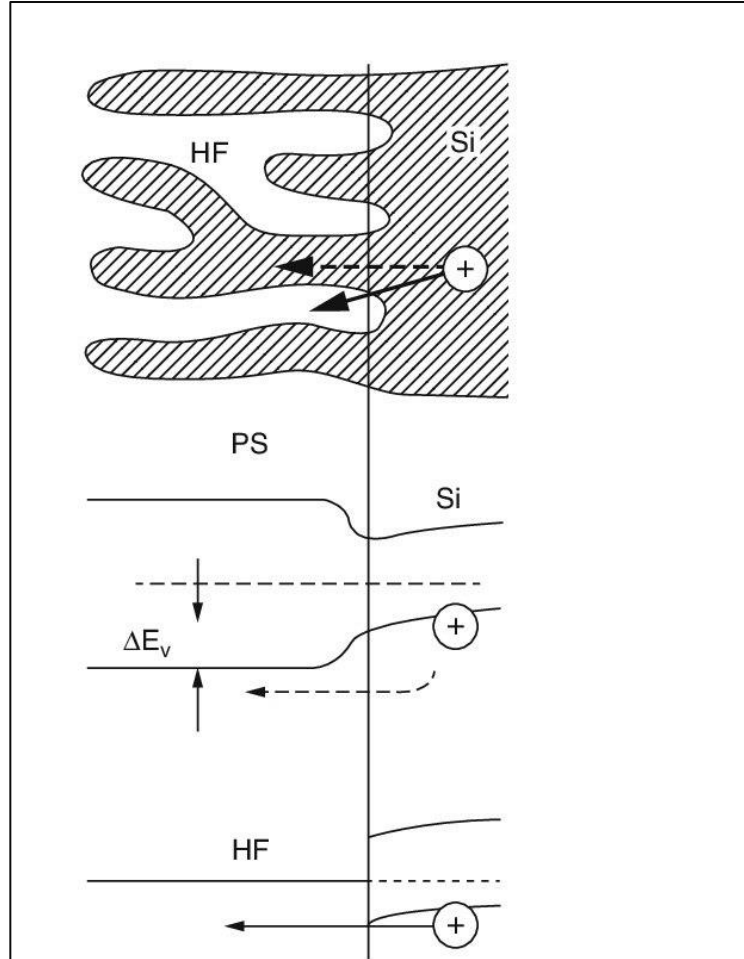
1.4.2.1. Electrochemical Etching

Electrochemical etching of Si in a solution of fluoridric acid and water or ethanol can produce porous Si. Porous Si can also be created by dissolving Si in ethanol with HF. This electrochemical method was first developed for the purpose of electro-polishing silicon wafers. If the current is low enough, electro polishing will not take place, and a regime will be established in which a random network of micro pathways penetrating the Si will be produced. This regime is one that has the characteristic of producing porous silicon. As a consequence of this, a layer in the silicon wafer that resembles a sponge and is made up of both porous and crystalline components is produced [33].

The pore sizes created by electrochemical etching of silicon in different electrolytes can be tailored to be anywhere from 1 to 10 nm, the electrochemical etching device made a silicon wafer, utilizing ethanol and aqueous HF in combination to create porous silicon film, A 1: 1 mixture (48% HF: ethanol) is created [which is the etching solution]; this mixture is then used to produce porous silicon film. In this method, aqueous HF solutions with constant current densities between 1 and 300 mA/cm² are used to turn silicon into a material with a large surface area. This is the most common way to prepare Ps [34].

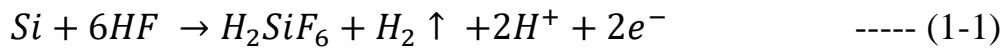
A charge transfer occurs at the interface of the semiconductor and the electrolyte when a silicon wafer is immersed in a solution containing electron acceptor species; Figure (1-3), shows Schematic of the Porous Silicon and bulk silicon interface (top) and band diagrams for charge transfer from the bulk to the porous skeleton (middle) and from the bulk

to the electrolyte at the pore tip (bottom). Hole change at the end of the pore is energetically favorable compared to pore wall transition (broken arrow).



Figure(1-3) Schematic of the interface between Porous Silicon and bulk silicon.

The following is a proposed chemical reaction and its description:



Since H_2SiF_6 or some of its ionized forms are the finished and reliable silicon product in HF, this means that just two of the four silicon electrons are available. take part in an interface modification transmission during pore formation, while the other two undergo hydrogen production due to corrosion [35].

1.4.2.2. Stain Etching Technique

Stain etching is also another way to create films with a high proportion of anodically processed (Ps) material.

When making (Ps) films, standard etching procedure for the use of nitric and HF acids. HF: HNO₃: H₂O is the most typical stain etching etchant. After a pause of one or two minutes (the "incubation time"), the etching process begins. It has been determined that the incubation time for P-type samples grows longer as sample resistivity rises, falling somewhere between 8 and 10 minutes [36]. The stain etching reaction of silicon can be expressed as [37]:



The stain etching technique is an amazing option in (Ps) formation due to the inherent simplicity of the fabrication procedures; nevertheless, this method is also considered to be really slow, and the top of the Ps layer that is made is very rough. It is especially advantageous in situations in which extremely thin Ps sheets with uniform depth (101–102 nm) are required; Stain-etched porous silicon films feature visible photoluminescence and are thinner than anodized films [38].

1.4.2.3. Electrophotochemical Etching

Since both N- and P-type silicon may be etched using HF solution, this technology is regarded as crucial in the (Ps) material sector.

The electrophotochemical etching procedure is advantageous because it combines the best features of etching by electrochemistry and photochemistry. have reported that lighting of P-type and N-type Ps During the creation produces significant alterations in the layer structure of both types. In order to produce N-type (Ps) under light, the PEC

etching technique uses a layer of nonporous silicon to cover a layer of macroporous silicon with pores on the micron scale [39].

1.4.2.4. Etching Done with Photochemicals

Electrochemical wet etching in hydrofluoric (HF) solution has resulted in naturally porous silicon. At the silicon-electrolyte interface, n-type silicon forms a space-charge zone, which in turn creates a built-in potential. As the potential at the interface attracts holes from the valance band, a chain reaction of etching can begin if there are enough holes. How? By passing a current or potential between two electrodes. Without the need for electrodes, light may be used to create the necessary holes and set the device's internal potential to any value. As stated by Noguchi et al. This method employs photon sources like lasers and intense light to create the necessary holes in the area that was irradiated of the silicon chip at the outset of the etching process [40].

The benefits of etching using photochemistry, which has been used to create (Ps) and silicon nano crystallites, are as follows; The Steps are Straightforward (without external potential); more precise processing parameters that can be controlled and regulated; slow etching and uneven lighting are just two of the problems with this approach. Overall, the layer thickness and surface morphology of the (Ps) structure created via the photochemical etching method vary with the wavelength and intensity of the light used in the procedure [41].

1.5. Porous Silicon's Unique Characteristics

The amazing qualities of the porous silicon (Ps) layer have led to its employment in a diverse array of settings.

1.5.1 The Chemical Characteristics

According to Andria, High specific surface area of the (Ps) layer (which ranges from 200 to 600 m²/cm³) has been shown to have an effect on chemical characteristics, which in turn will have an impact on the optical, electrical, and mechanical attributes of the (Ps) layer [42].

The chemical properties of freshly etched silicon samples are particularly sensitive to the local ambient, where they change over time while being stored in air, due to the high density of dangling silicon bonds with original impurities like hydrogen and fluorine, which are remnants from the electrolyte. This is due to the high density of dangerous silicon bonds with initial contaminants like fluorine and hydrogen on the pore surface [43].

The surface chemical composition of the (Ps) layer was studied by using X-ray photoelectron spectroscopy and Fourier transform infrared (FTIR) spectroscopy. The FTIR signal from the (Ps) layer is substantially stronger and easier to quantify than that from bulk silicon due to the large specific field [44].

1.5.2. The Physical Characteristics

Important considerations in defining the physical properties of porous silicon include the size and form of the holes, the thickness and proportional Si content, the presence of voids, and, in some situations, the proportional amounts of different Si molecules in the porous material that was generated. These variables are dependent on the preparation circumstances and allow the creation of materials with physical characteristics similar to those of silicon and air (or the medium, which fills the pores). Additionally, (Ps) becomes substantially more exciting

when the function size of Si wires is less than just few nanometers due to the emergence of other quantum-size features. Over the past two decades, (Ps) had also gained popularity by many scientists and engineers due to its adaptability and durability, and it has been used in a variety of industries [45] [46].

1.5.3. Porous Silicon Structure

Studying the morphological and X-ray diffraction features of porous silicon is essential for understanding its structure. Pore type, shape, and size are only a few of the structural of the measuring features layers made of porous silicon that are unique to their production circumstances [47].

1.5.3.1. The X-Ray Diffraction

X-ray diffraction (XRD) is a flexible and non-damaging way to determine the fact that different microstructures and phases using a diffraction-based experiment of those structures and phases being exposed to x-rays of a specific wavelength. This method was developed in the 1940s by the American Institute of Physics. Each unique phase structure can only cause a change in the path an incident x-ray takes when the angle of incidence falls within a specific range, which can then be determined [48]. Nanoscale crystals are incorporated into the structure of the transparent silicon. Numerous researchers have focused their attention on this property due to the significant impact it has on all of the properties of the porous silicon substrate. For porous silicon layers, Hauser et al. obtained x-ray diffraction data, demonstrating that despite the presence of a significant peak broadening, the Si material retains its crystalline structure [49]. This phenomenon is interpreted as a result of the nano crystallite size (see figure).

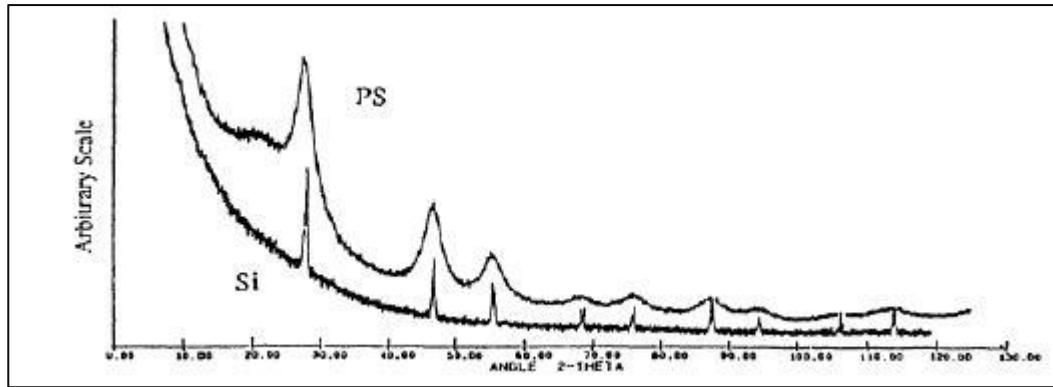


Figure (1-4), Bulk Si and Porous silicon X-Ray Diffraction [50].

1.5.3.2. Morphological Features

The structure of the pore medium has various morphological, geometrical, and metrical features such the size, shape, and arrangement of pores based on the preparation circumstances.

1.5.3.2. a. Pore Type

As shown in Figure (1-5), a silicon wafer's porous layer can have a wide variety of pore types . In the broadest meaning, a pore is a deep etch pit that surpasses its breadth, as in Figure (1-5, a). Distinct pores in Figure (1-5, b) are often closed at one end and entangled to some degree. In Figure (1-5, b), the majority of a few micrometers thick, there are layers of porous silicon, and each pore is usually closed at one end (1-5, c). The most common techniques for pore investigation, High resolution transmission electron microscopy (HRTEM) and High resolution scanning electron microscopy (HRSEM) are two types of high-resolution electron microscopy . Capping or thermally-induced reconstruction of the pore network can be used to make pores that are closed at both ends, as in Figure (1-5, d). Pores that have both ends open, as depicted in Fig (1-5, e), can be created in Ps membranes through capping or repair of the pore network caused by heat. Structures made by anodizing wafers for a long time or anodizing areas that have already been thinned, or "lift-off" approach of Turner. In latter situation, current is increased sufficiently to enter the electro polishing mode, resulting in the separation of the porous over layer from its foundation [51].

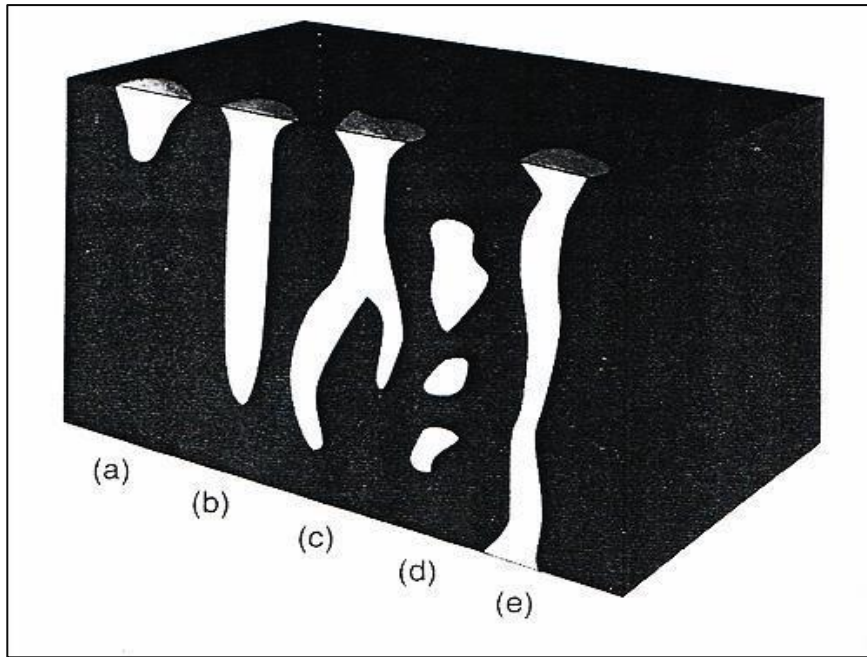


Figure (1-5), Types of pores: (a, b) Blind, Dead end. (c) Interconnected or Branched. (d) Totally isolated or Closed and (e) Through pores.

1.5.3.2.b. Pore Size

Pore size largely determines the optical and electrical characteristics of porous silicon[52]. The pore range in size according to the International Union of Pure and Applied Chemistry (IUPAC) are presented in Table 2.1. Given the quantum confinement effect of porous silicon, the great majority of electrochemically etched luminescent silicon studied to date is mesoporous [53].

Table (1.1); IUPAC Classifies Pores Based on Size.

Pore Width (nm)	Type of pore
≤ 2	Micro
2 – 50	Meso
> 50	Macro

1.5.3.2. c. Pore Form

Figure (1-6) is a sketch of the main types of pore shapes that have been reported for silicon, and that have been etched electrochemically. By furthermolre, the most prevalent form is that of a cylinder, as seen in Figure (1-6, a), with different amounts of "branching," as shown in Figure (1-6, c), and necking, as shown in Figure (1-6, d). Early Japanese studies showed that the layer looked like a "ink bottle," as shown in Figure (1-6, b) [54], with a thin surface porous film (SPF) that had pores that were much smaller than the rest of the layer. This kind of shape doesn't show up in mesoporous materials, but it can happen in layers with a lot of pores. As Zhang's SEM data make very clear, Most of the time, the pores in mesoporous materials tend to get smaller as you go deeper into the thick layers. This happens because The layer's top is subjected to the etchant for a longer period of time than the layer's bottom [55].

Crystallography also has a clear effect on the shape of pores, at least for macropores and large mesopores. Figure (1-6, d) shows that anodizing (100)-oriented wafers, it makes pores with a cross-section of a square, while anodizing (111)-oriented wafers can make pores with a triangular cross-section (1-6, e) [56] .

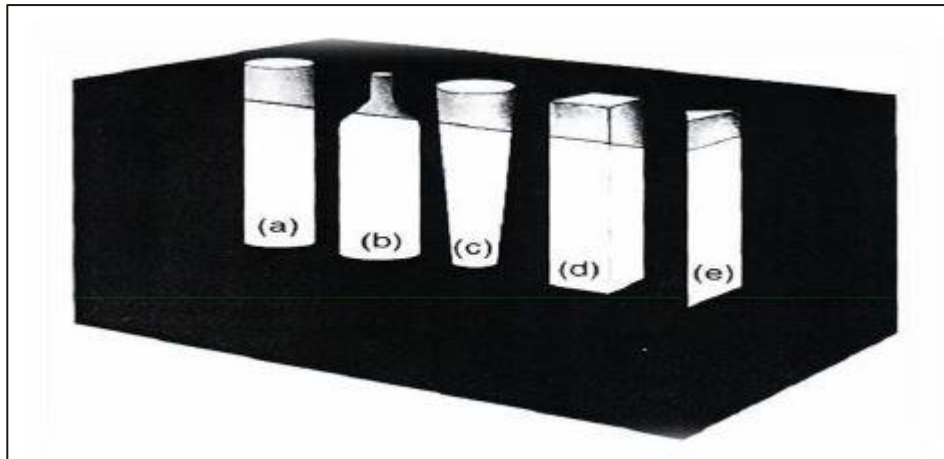


Figure (1-6); Pore shapes: (a) Cylindrical (b) Ink-bottle (c) Funnel (d) Cuboid or slit and (e) Triangular or Pyramidal.

1.5.3.2.d. The Porosity

The level of porosity in the porous silicon is the single most important defining characteristic of this material. It is referred to in terms of the proportion of vacant space within the porous layer, and it is simple to calculate by taking measurements of the layer of silicon prior to and after etching phase (m_1 , m_2). Moreover, following the removal of the porous silicon layer (m_3) with a molar solution of either KOH or NaOH.

The porosity may be found by using the following equation [57].

$$P = \frac{m_1 - m_2}{m_1 - m_3} \quad \text{----(1-1)}$$

m_1 : Weight of the samples before the process of etching.

m_2 : Weight of the samples after the process of etching

m_3 : Weight of the samples After taking off the Ps layer,.

1.5.3.2.e. The Surface Area

The surface area of porous silicon films is often described as the accessible area of solid surface per unit mass of material. This is because

porous silicon films have a very open structure. The scanning electron micrograph reveals that porous silicon is made up of a complex network of pores and columns that are nanometers in size and are separated by very thin walls. These structures have a very large surface area, which typically ranges from three hundred to six hundred square millimeters per cubic centimeter and is dependent on the experimental conditions. Surface area has a significant impact on a number of characteristics, including those of materials made of micrometer-sized grains and those exposed to nanometer-sized particles. These qualities include: For instance, the electrical resistivity of granular material is anticipated to increase proportionally with the total number of grain boundaries [58] [59].

The surface volume ratio (specific surface area), which may be measured in m^2 / cm^3 , could be calculated by using the equation below:

Surface Area(m^2 / cm^3) = Area of one pore No.of pores / (Area of Ps structure Depth) [60].

since the pore geometry is assumed to be cylindrical in shape and thus the area of one pore is

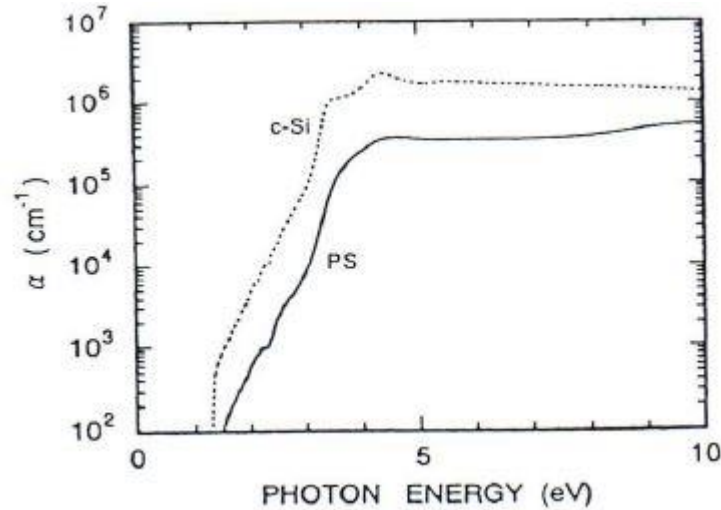
$$\text{One pore's area} = 2\pi r_{\text{Ps}} h_{\text{Ps}} \quad \text{----(1-2)}$$

The height of the pore, in meters, is denoted by h_{Ps} ,

while the pore's radius, in units of area, is denoted by r_{Ps} (m) [61].

1.5.4. Optical Characteristics

Nano crystals' optical absorption edges shift to the blue due to quantum confinement phenomena, in comparison to bulk silicon. Porous Si has a smaller absorbance value than bulk Si, as seen in Fig (1-7).



Figure(1-7) Absorption Coefficient of Crystalline Silicon and (Ps) [62]

The quantum confinement energies of electrons and holes have an effect on the absorption edge of band transitions from one band to the next.

Due to the reduction in dimensionality, the relative permittivity(ϵ_{pore}) of (Ps) and, as a result, the refractive index (n_{Ps}) are altered. This is because The columnar crystalline silicon particles that make up the silicon at the nanoscale are spread apart by air. As a result, The Bergman's effective medium estimate says that the ϵ_{Ps} is linked to the porosity (P).

$$\epsilon_{\text{Ps}} = \epsilon_{\text{si}} - P (\epsilon_{\text{si}} - \epsilon_{\text{pore}}) \quad \text{---(1-3)}$$

Silicon has a relative permittivity of (ϵ_{si}), while air has a relative permittivity of (ϵ_{pore}). Since it is expected that the refractive index (n_{Ps}) will be lower than that of crystalline silicon and will go down as the porosity goes up, When the porosity is higher, the relative permittivity of porous silicon is lower than that of crystalline bulk silicon [63].

The effective dielectric function's square root can be used to calculate the refractive index [64]:

$$n_{ps} = \sqrt{\epsilon_{ps}} \text{ ----(1-4)}$$

1.5.5. Electrical Capacitance of a Silicon layer with pores

It is possible to learn a lot about the electrical characteristics of (Ps) layers and the instruments that employ them by measuring their capacitance. Capacitance tests reveal information about the M/Ps/c-Si/M sandwich structure, including the built-in potential, depletion layer width, and effective carrier density [65].

As can be observed in Figure (1-8), the capacitance of a (Ps) layer decreases with increasing layer thickness and porosity, both of which are dictated by the layer's morphological features .

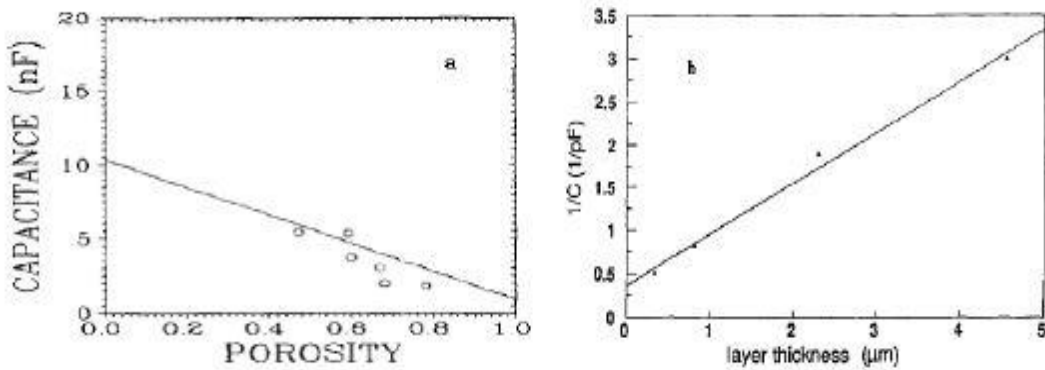


Figure (1-8) Capacitance of Ps layers (a) Porosity & (b) Layer thickness [66].

One may use this equation to calculate the capacity of the (Ps) C_{Ps} (F) layer [67]:

$$cpsi = A * (\epsilon_{ps} * \epsilon_0) / d \text{ ----(1-5)}$$

A (cm²) : the (Ps) layer's surface area.

d (cm) : the thickness of the (Ps) layer.

ϵ_0 (F/cm) is the relative free space permittivity and ϵ_{Ps} is relative permittivity of (Ps).

1.6. Extensive Use of Porous Silicon

A dielectric substrate with many different applications is porous silicon. Due to its designable material characteristics, compliance with classic Si manufacturing and thin film methods, as well as its particular qualities, both chemical and physical [68].

The prospective uses of porous silicon are tableted in Table (2-3), which also provides an overview of the characteristics of porous silicon that are required for each use case.

Table (1-2) Application of Porous Silicon [69].

Application area	Role of porous silicon	Key property
Optoelectronics	LED	Efficient electroluminescence
	Waveguide	Tunability of refractive index
	Field emitter	Hot carrier emission
	Optical memory	Non-linear properties
Micro-optics	Fabry-Pérot Filters	Refractive index modulation
	Photonic bandgap structures	Regular macropore array
	All optical switching	Highly non-linear properties
Energy conversion	Antireflection coatings	Low refractive index
	Photo-electrochemical cells	Photocorrosion cells
Environmental monitoring	Gas sensing	Ambient sensitive properties
Microelectronics	Micro-capacitor	High specific surface area
	Insulator layer	High resistance
	Low-k material	Electrical properties
Wafer technology	Buffer layer in heteroepitaxy	Variable lattice parameter
	SOI wafers	High etching selectivity
Micromachining	Thick sacrificial layer	Highly controllable etching
Biotechnology	Tissue bonding	Tunable chemical reactivity
	Biosensor	Enzyme immobilization

1.7. Hydrogen Fluoride

The chemical substance with the formula (HF) is hydrofluoric acid, and it is the primary source of fluorine used in industry. Therefore, it is regarded the precursor of several essential chemicals such as pharmaceuticals and polymers (including Teflon). hydrogen fluoride is frequently utilized in the sector of petrochemicals and as an ingredient in a number of super acids . Hydrogen fluoride is unique among hydrogen halides in that it boils at a low temp than room temperature while the others is condensed [70].

One of the hybrid orbitals (2pz) in the molecule (HF) is occupied by the single hydrogen atom's covalent bond (sigma) to the fluorine atom; the other three orbitals are filled with fluorine atoms (2px , 2py additional to 2s). Each of orbitals may accommodate 3 electron pairs. Hydrogen fluoride's theoretical molecular structure, looks like what's depicted in Figure (1-9). Hydrofluoric acid (HF) is one of the acids that reacts the most quickly, yet it is misunderstood as a weak acid due to the high electronegativity of fluorine. The acid's high electronegativity means that it is reluctant to give up its lone hydrogen, and because the ionization of an acid diminishes with its capacity to relinquish hydrogen, this acid is weak [71].

Hydrofluoric acid (HF), although being one of the most reactive acids with a fast rate of reaction, is considered to be a weak acid due to the strong electronegativity of fluorine that it contains. Because the acid has a high electronegativity, it doesn't readily give up its only hydrogen. As we are aware, the ionization of acid goes down as its ability to give off hydrogen goes up. consequently, the acid is considered to have a low concentration of hydrogen ions and a low ionization potential [72].

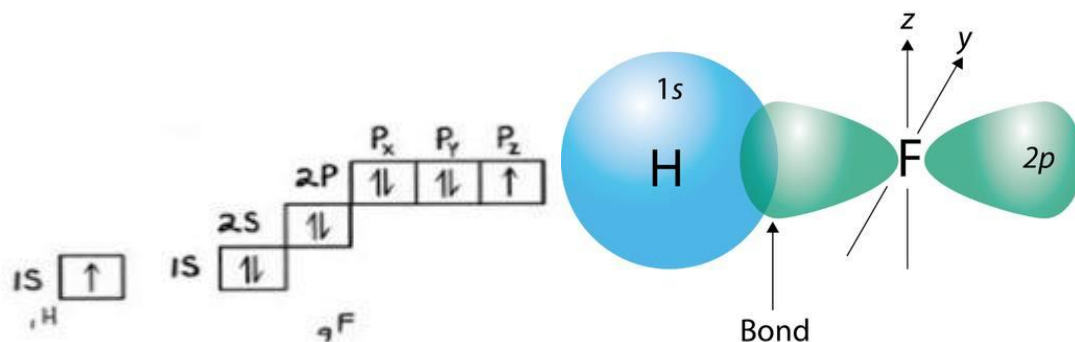


Figure (1-9) Hybridization of HF.

1.8. Historical Review

In 1956, Arthur Uhlir at Bell Phone Laboratories was working on electrochemical (EC) etching of silicon using a solution of hydrofluoric acid (HF). This was done with the intention of polishing and shaping micro-structures in silicon [73].

The first application of phosphorus sulfide in electronics was demonstrated in 1971 by Watanabe and Sakai. This application was the so-called complete isolation by the porous oxidized Si process (FIPOS), in which Ps layers were used to isolate the device in integrated circuits; however, contemporary research showed a low reduction [74].

In the 1970s and 1980s the interest in porous silicon increased because the high surface area of porous silicon was found to be useful as model of the crystalline silicon surface in spectroscopic studies [75].

The level of interest in this topic did not change significantly until the beginning of 1990, when Leigh Canham's discovery of room-temperature image and Ps electroluminescence advanced research due to the enormous potential in silicon-based integrated optoelectronics applications. Prior to that time, the level of interest in this topic remained relatively stable. Within a short period of time, the number of publications experienced a rapid growth. These publications included studies that

discussed numerous uses of Ps, as well as manufacturing techniques, physical qualities, and chemical features [76] [77].

The first model to explain the mechanism of Ps layer formation was reported in 1991 by Lehmann et al[78] .

Lang, et al. In1995, made porous silicon from doped foil crystals of silicon using three distinct light aided conditions (violet, visible, ultra and dark light) [79].

In 1998, Lee Kanham published the results on the red luster of porous silicon, which was described in terms of the quantitative confinement of the carriers in the silicon nanocrystals that were present in the pore walls. These nanocrystals were found in the pore walls. Since that point in time, the interest of academics and technicians in this material (as well as other porous semiconductors as well) has been continually expanding, and the number of papers that are dedicated to this category of materials is growing every year. An explosion of effort focusing on the creation of silicon-based optoelectronic switches, displays, and lasers occurred once it was discovered that porous silicon can effectively emit visible light. This discovery led to the explosion. Over the course of the previous two decades, research into the optical characteristics of porous silicon has reached a very high level of activity [80] [75].

In 2001, 2005, and 2006, D.G. Rasheed and its groups conducted experiments demonstrating that (Ps) may be manufactured with laser assistance via a method known as laser-induced etching, which results in a material with a number of desirable structural and optical features [73].

In 2006, a team of researchers looked at how the morphology of porous silicon changed depending on the preparation conditions [81].

In 2008, Ps shows that there is a steady change over time. Different oxidation/passivation processes for Ps structures have been suggested to avoid the temporary aging period. Both partial oxidation (also called "pre-oxidation") and full oxidation (also called "oxidation") are used in optical applications like optical waveguides, image detectors, dielectric filters, and photoluminescent components . In this year also, Izabella looked into the use of porous silicon in solar cells, a field that requires the use of one-dimensional photonic crystals [82] [56].

In 2009, by using electrochemical etching, Nansheng was able to produce a porous silicon layer that acted as the emitter layer of a solar cell with unprecedentedly low reflectance. Altering the electrochemical conditions allows for straightforward control over the (Ps) layer's shape and reflectivity (current density and etching time) [83].

In 2010, the morphological characteristics of porous silicon and oxidized porous silicon formed by photo-electro-chemical etching from an n-type silicon wafer have been described by Alwan M.Alwan et al. as a function of experimental circumstances[84].

In 2012, Ahmed K.AL-Kadumi investigate the properties of nanostructured Ps that has been created through photo-electrochemical etching [63].

In 2021, Noor.M , Hamida.I and Ahmad k.Al-Kadumi , research should be done on the Properties of Ps for both P-type and N-type Bulk Silicon [67].

Aims of Study

- 1- Study the creation of porous silicon from bulk silicon using three solutions (HF + Ethanol , HF + HNO₃ and HNO₃ + Salt), by using electrochemical etching process in different times (5-10-15-20-25-30) minute.
- 2- Study the characteristics of electrochemically etched porous silicon.
- 3- Investigating the behavior of porous silicon in Hydrofluoric acid and ethanol.
- 4- Analysis the response of porous silicon's to hydrofluoric and Nitric acids.
- 5- Quantifying the porosity, layer thickness, refractive index, relative permittivity, and capacitance of porous silicon and compare results.

Chapter Two

Experimental part

2.1. Introduction

This section provides a description of all of the apparatuses and instruments (See table 2.1) have been used in the process of making layers of porous, in addition the techniques already utilized to research and explain the properties of (Ps) layers. Additionally, this chapter examined the techniques that have been used to research and explain the features of (Ps) layers.

2.2. The Materials and Equipment Utilized in This Research

Table (2.1) The Equipment's Utilized in the Research

The Devices Name	Type of Device and Manufacturer	Work Place
x- Ray Diffraction instrument	Philips- PW1730	University of Tehran
Device Power Supply (DC)	YX- 1501 AD - China	University of Kerbala
Scanning Electron Microscopy (SEM)	MIRA3 TESCAN Det: In Beam	University of Tehran
Sensitive Electrical Balance	Lab-BL210, Sartorius - in Germany	University of Kerbala

Table (2.2) Shows the Materials Used

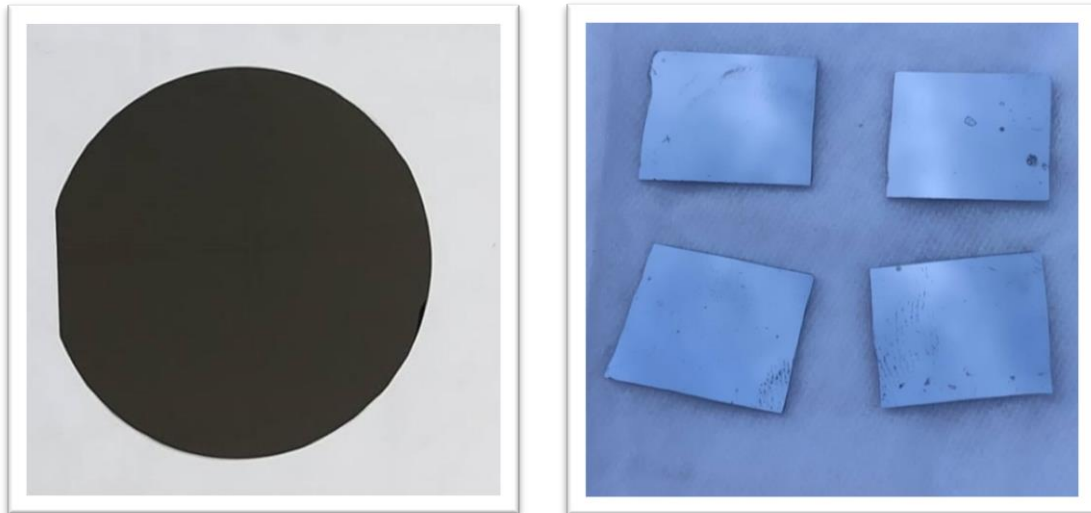
Topic Identifier	Chemical Components	% and purity	The Manufacturing company
Wafer silicon P-type	Si	99 %	California, United State
Nitric Acid	HNO ₃	70%	Thomas Baker-India
Hydrofluoric Acid	HF	39-43%	New Delhi - 110002(India)
Ethanol	C ₂ H ₅ OH	99.9%	Nether Lands
Potassium Hydroxide	KOH	85 %	Mumbai – India

2.3. Preparation of Samples

This content includes description of all devices and equipment that were used to make the Ps layers. in addition the techniques that were used to study and explanation the properties of the ps layer.

In this work, porous silicon is products using electrochemical etching of p-type (111) oriented bulk silicon wafer and diameter: 12.5cm, thickness:575 μm , Resistivity: 1-10 $\Omega\cdot\text{cm}$, California , United State .

In figure (2-1), a silicon wafer is seen being sliced to the dimensions(1.5*1.4)cm (2-1, b).



(a)

(b)

Figure (2-1) Wafer photo (a) Prior to cutting the bulk silicon (b) After a silicon-cutting.

Following the preparation of the samples (bulk silicon after cutting), they were then divided into three groups, with each group receiving a distinct solution from the set of three solutions that were employed. The began with the first solution, which consisted of nitric acid mixed with salt.

These pieces was laundering with ethanol to remove dirt by mixture ethanol and HF acid (10%), the sample is placed within the system (figure 2-2), in the setup diagram for the porous electrochemical etching, A sample has been placed on top of a Teflon cell such that no current can travel through the back surface. To create Ps layers, in a parallel electrical circuit, a silicon electrode served as the anode and a platinum electrode served as the cathode.

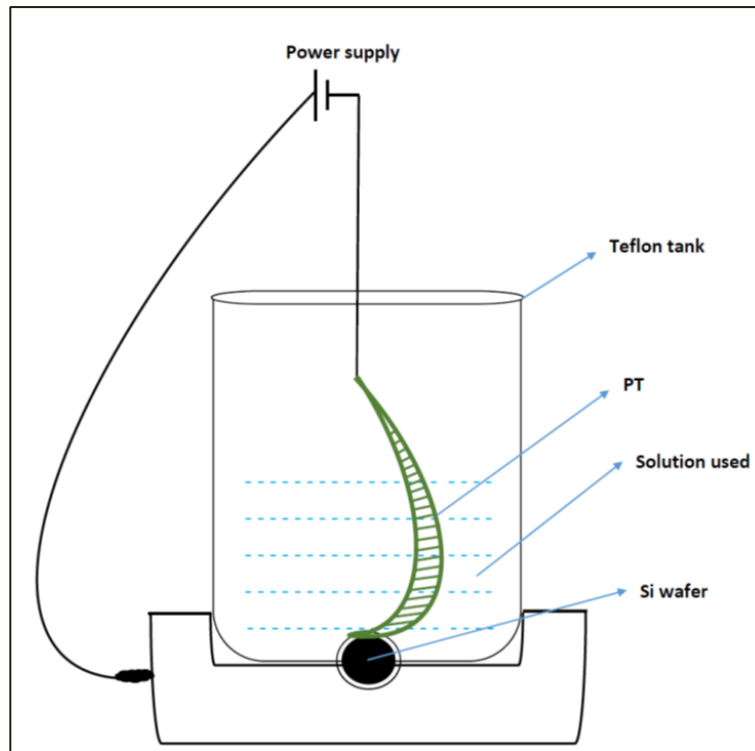


Figure (2-2), The Systematic for Electrochemical etching which used in this study.

Next, the active device is turned on, and put the solution on it. Finally, we repeat these processes at various periods throughout the course of (5,10,15,20,25 and 30) minutes.

In order to investigate the characteristics of porous silicon, each time there is a total of four samples created. After the allotted amount of time has passed for each sample, it is removed from the system, rinsed with distilled water, and then placed inside a plastic tube that has ethanol in it to prevent it from oxidizing. This step is done in order to keep the sample from being contaminated, one can be noted in figure (3-3).



Figure (2-3), Real image for using the ethanol as storied solution for sample.

After that, all of the procedures are repeated for the remainder of the solutions, which are hydrofluoric acid and nitric acid, and the final solution is hydrofluoric acid and ethanol, and all of the work was done in a careful environment owing to the hazards posed by the acids that were utilized.

2.4. The Measurements

Following these readings, the layer's composition (Ps) was determined:

24.1. Gravimetric Measurements

To determine the porosity and layer thickness of the (Ps) layer, the weight of the samples prior to and after the etching process, as well as the weight of the sample after the removal of the (Ps) layer from the sample (figure 2-4) , by immersing for an extended period of time, were weighed

and compared (30min). In KOH (1M) , which was made by mixing 14 grams of KOH and 250 milliliters of D.W [85].

$$M = \frac{wt}{M.wt} * \frac{1000}{Vml} \quad \text{----(2-1).}$$

Following the gravimetric measurement, the thickness of the porous layer, denoted by the letter d, may be calculated using a variety of methods.

Then using equation (2-2) to compute layer thickness (d) [86] .

$$d=(W_1- W_2) / (\rho s) \quad \text{----(2-2)}$$

Where W_1 The sample weight before etching, W_2 The sample's weight after etching, ρ is silicon density (2.3 g/cm^3) and $S \text{ (cm}^3\text{)}$ is the etched surface area.



Figure (2-4), Real image when Porous layer was removing in KOH.

The exit of bubbles indicates the release of hydrogen gas due to the demolition and removal of the nanostructure

2.4.2. Optical Measurements

Porosity and the constants $\epsilon_{\text{si}}=11.68$ and $\epsilon_{\text{pore}}=1$ are used in the equation (1-3) to derive the relative permittivity, and The square root of the relative permittivity is used in the equation to find the refractive index [87].

$$n_{PS} = \sqrt{\epsilon_{PS}} \quad \text{--- (2-3)}$$

2.4.3. Rate of Etching Measurements

By taking the layer thickness and the etching duration (5,10,15,20,25 and 30 minutes), one can derive the etching rate [88]:

$$V = \frac{d}{t} \quad \text{----(2-4)}$$

V : The etching rate (cm/min)

d : Layer thickness of Porous silicon(cm)

t : Etching time (min)

2.4.4. Measurement of Porous Silicon's Electrical Capacitance

By first measuring the relative permittivity, which can be shown to be connected as a function of layer thickness for porous silicon by using the equation, it is feasible to calculate the capacitance of porous silicon (1-6)

2.4.5. The X-Ray Diffraction Technique

In this work, the morphological characteristics of porous silicon (Ps) layers, including their nanocrystallite size, crystalline or amorphous structure, and small constant, have been studied. This research was conducted at Tehran University. and utilized an X-ray device manufactured by Philips and supplied by the company.

2.4.6. The Scanning Electron Microscope (SEM)

Taking a direct picture of the Ps layer, The Ps layer's structural measurements are performed utilizing a field emission scanning electron microscope. Utilizing computer simulations, morphological characteristics of the Ps layer, such as pore size, pore shape, and wall thickness between pores, are investigated (SEM) At the university in Tehran, the spectroscopic electron microscopy (SEM) observations are performed using the parameters EHT=15.00kv and signal A=SE₂.

Chapter Three

Results and Discussion

3.1. Introduction

As a result of these applications reflect to the micro crystalline qualities of Si, examples include photovoltaic cells and gas detectors, the porous silicon attributes are particularly essential in relation to the applications. Porous silicon may be used to make gas sensors and solar cells [89].

In this portion, the characteristics of porous silicon that were created by electrochemical etching for P-type processes on nanocrystalline silicon substrates are shown and discussed. These features were fabricated using nanocrystalline silicon as the base material Ps layer structure, morphology, optics, and electronics were investigated, as were the findings that one may characterize in this way.

3.2. Structure Properties in a Layer of Porous Silicon

The layer of Ps is a particularly special structure that may be identified by presence of interconnected a single crystal's pores. This gives layer its name. The prepared layer's morphological characteristics, including its surface area, porous, layer thickness, hole depth, hole shape, wall thickness between pores (Were examined) and shape of the (Ps) layer, which can be size of the Nanoscale crystallites, whether they are crystalline or amorphous, are both strongly impacted by the circumstances under which the etching is performed [90].

3.2.a. The Porosity

This section will examine the link between the porosity ratio of porous silicon and the various preparation timeframes.

Different results are obtained that are affected by the solution used, and through the experiments conducted. In this study has been used three solutions, first one is Nitric acid with HF , Ethanol with HF, last one is Nitric acid with salt (NaCl).

In Nitric acid with HF, it was determined that the pores on the silicone surface are stronger because its reaction is slow, as indicated by the fluctuation curve in Figure (3-1), whereas the ethanol solution with the HF is fast, so it is evident that the ethanol solution with the HF is more effective. As shown in figure (3-2), the porosity of the second solution is less than that of the first, indicating that the union of nitric solution and HF with silicon is stronger [91]. In general these figures are the porosity as a function of the etching time, In fig (3-1) that there is increasing in the porosity and tend to saturation, where as in fig (3-2) the porosity tend to decrease all this produced from the reaction techniques .

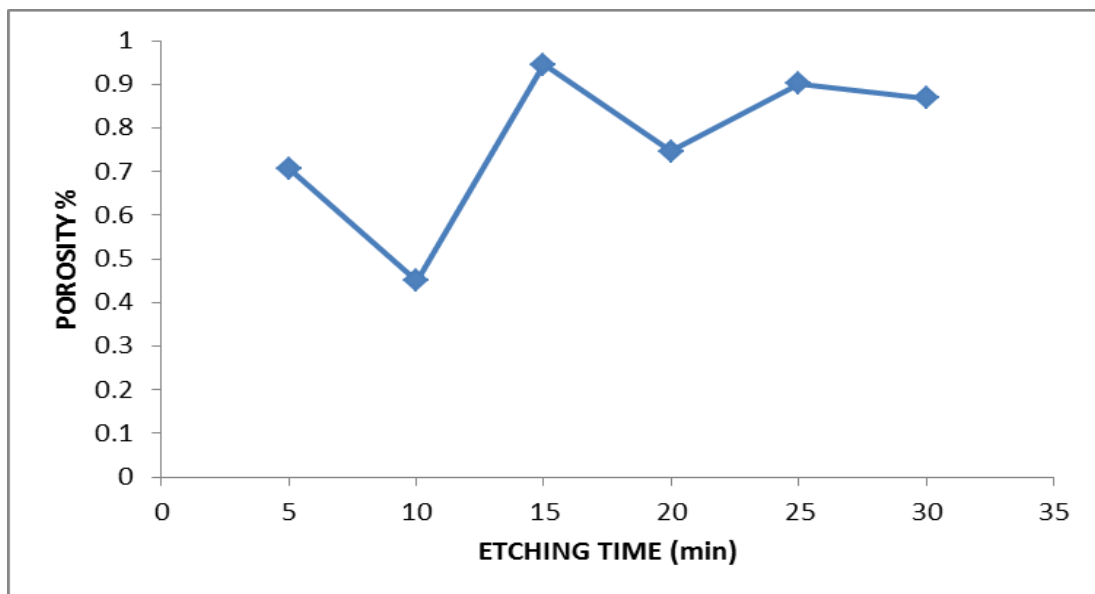


Figure (3-1) Relation between Porosity and Etching time for Nitric acid with HF .

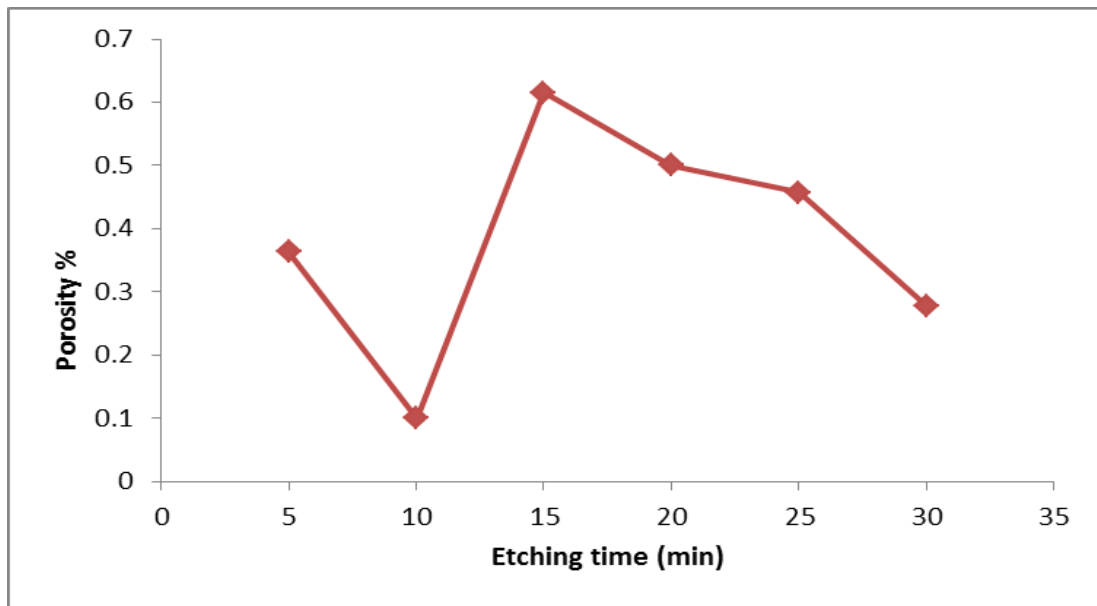


Figure (3-2) Relation between Porosity and Etching time for Ethanol with HF.

The porosity is the number of holes per unit area, and it was greater in the nitric solution due to the delayed reaction, thus the pores are well-drilled and seem strong, as seen in the figure (3-3).

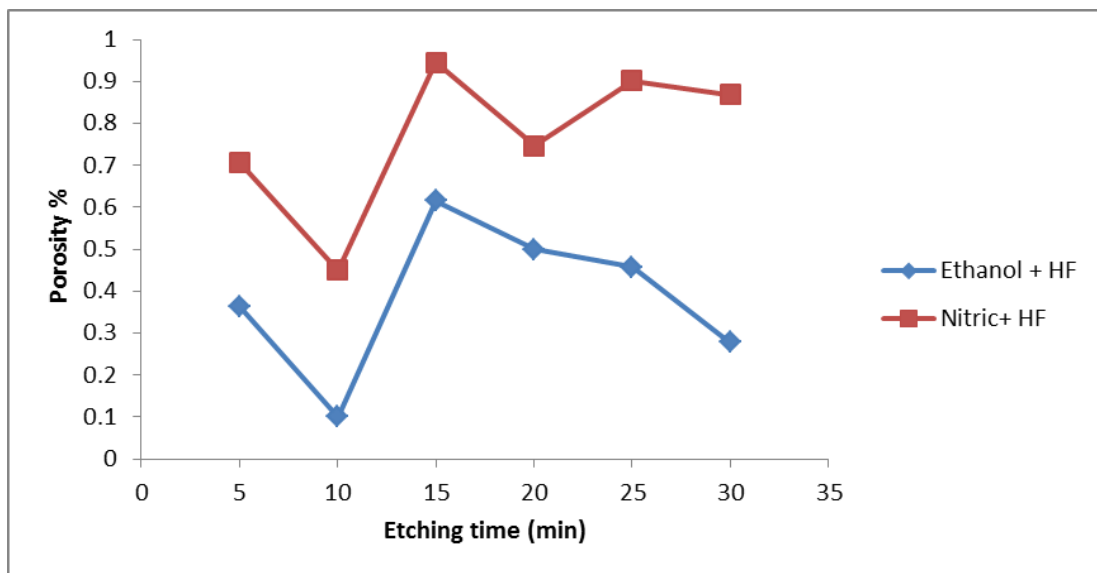
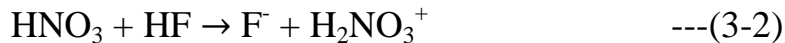
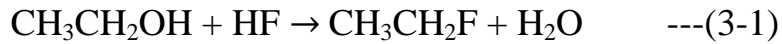


Figure (3-3) Relation between the Porosity and Etching time for both solutions.

Below, some equations that describe how the reaction should be carried out:



Because F^- is more basicity and electronegativity than OH^- ($\text{F} = 3.98$, $\text{OH} = 2.2$) .

HF and HNO_3 reaction slower because they are both acids and want to lose H^+ [92] [93].

3.2.b. Layer Thickness

Due to the fact that, as stated in equation, the etching rate is defined as the ratio between the thickness of the Ps layer and the etching time (2-3), The etching rate is directly related to the layer thickness [52].

When observing figure (3-4), it displays signals for ethanol and hydrofluoric acid samples. From this figure make some information about the structure of ps. the graph shows the number of layer thickness ranged 5-30 minutes. It is noticed that the thickness of the layer increased by 0.0002 (cm) at a time of five minutes, this is evidence of the structure of porous silicon, and in the 10 minutes the thickness of the layer decreased due to the fact that the powerful reaction causes the polishing and removal of the porous silicon layer [94].

This was followed by a dramatic rise to 0.0009 (cm) at 15 min indicator of very good porous silicon layer (formed a new Ps later); Then continues in fluctuate. multiple patterns of ethanol solution are observed over the etching time, where its reaction is fast and a porous layer is formed and then polishing occurs in a fast way, so the values of the thickness of the layer appear less, which indicates that the layer is smaller than it was before [95].

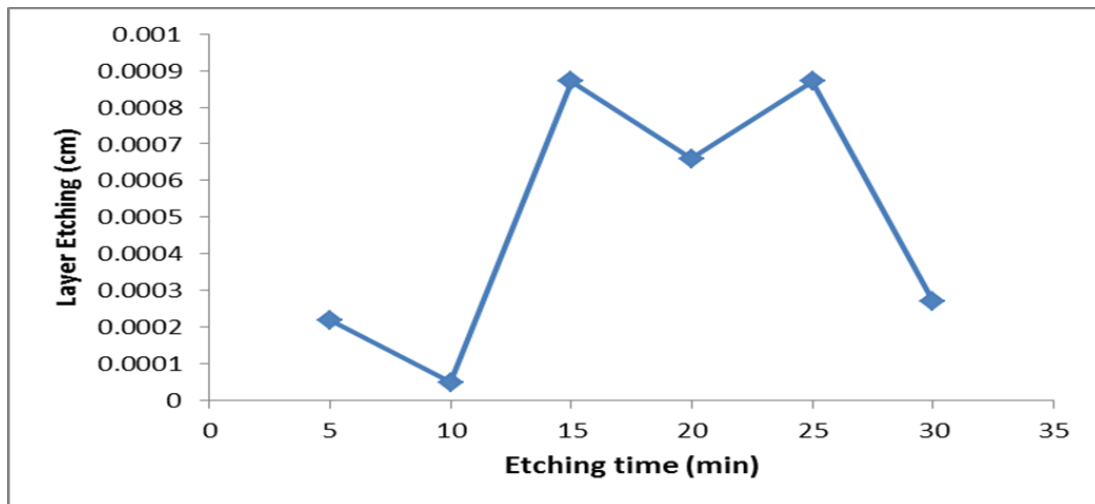


Figure (3-4) Relation between Layer Thickness and Etching Time for Ethanol with HF.

Figure (3-5), which shows that the highest value is reached in a time of 15 minutes and the reaction is in one pattern. However, when observing figure (3-5) [96], The layer that was produced as a result of the nitric solution due to the fact that the reaction of nitric is slower, resulting in the formation of the porous layer more frequently and maybe in the same pattern in most nitric reactions [97]. But in the reaction of ethanol with hydrofluoric acid, there is more diversity. As a result, the applications of porous silicon resulting from the reaction of ethanol are more widespread, whereas the porous silicon produced by the reaction of nitric is of higher quality. Accordingly, The reaction solution is used depending on the desired application of the porous silicon [98].

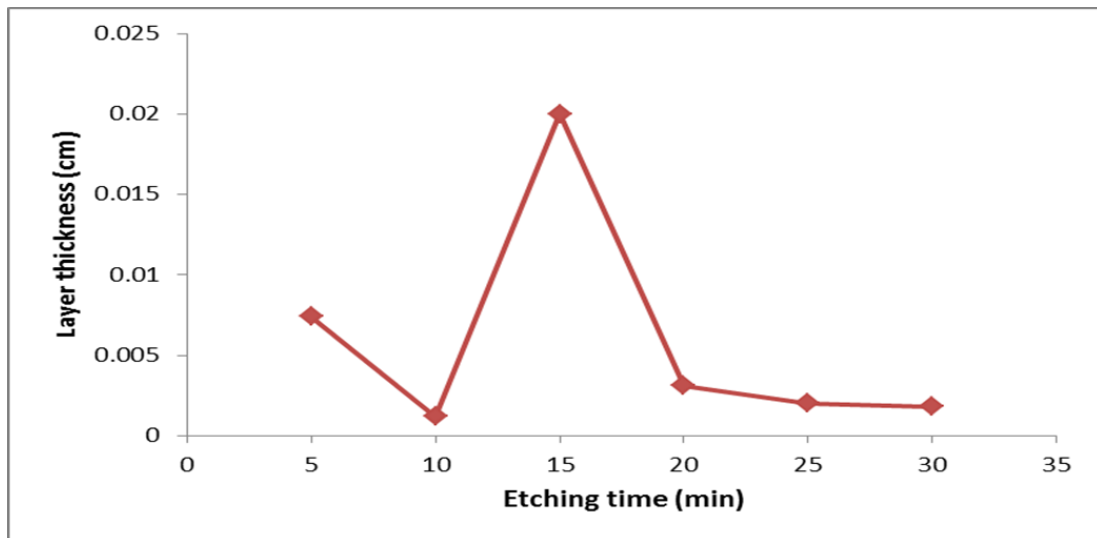


Figure (3-5) Relationship between Layer Thickness and Etching Time for Nitric acid with HF.

Furthermore, from figure (3-6) one can observe the thickness layer by using Ethanol + HF is constant in comparison of the Nitric acid +HF, Nitric acid +HF is high fluctuation [99] .

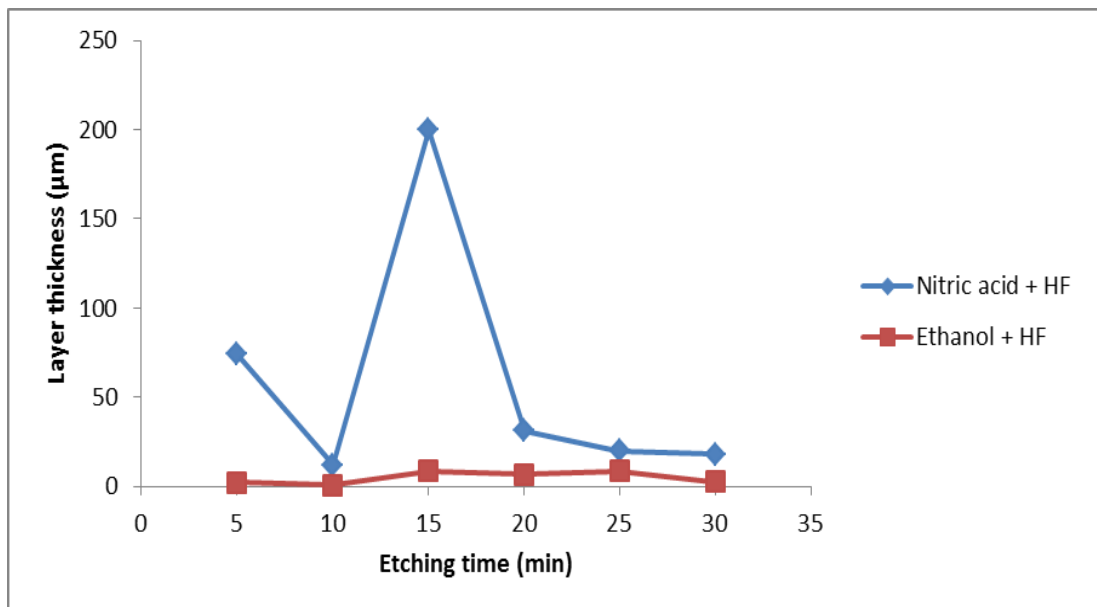


Figure (3-6) Relationship between Layer Thickness and Etching Time for both Solutions.

3.2.c. Scanning Electron Microscope (SEM)

The nano-porous silicon films that were created have pores of varying sizes and configurations. The top view (SEM) photos make it very easy to discern an array of blank spaces, which are black, and pores in the silicon matrix, which are brilliant.

The researchers are concentrating atop of Ps walls since those are the walls. the fundamental component of nanocrystalline silicon, which demonstrated the characteristics of quantum confinement effect.

Figure(3-7) displays that at 5 minutes, a scanning electron microscope image of the sample of HF and HNO₃ can be observed with etching time, It is possible to see in the five minutes, the Ps layer is in the process of forming. As time progressed, the porous layer did indeed form, as can be seen in the 25 minute sample in figure (3-8), It is plain to see that the porous layers are developing; and at the same time, nanowalls are coming into being. This sample has a nanoscale that measures 39.99 nm [100].

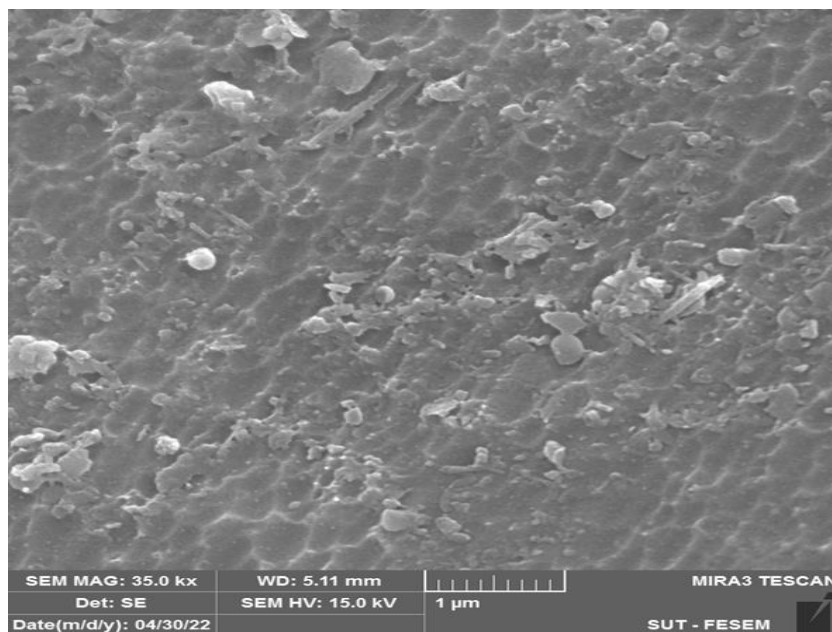


Figure (3-7) SEM Image of Ps layer with HNO₃+HF at 5 min.

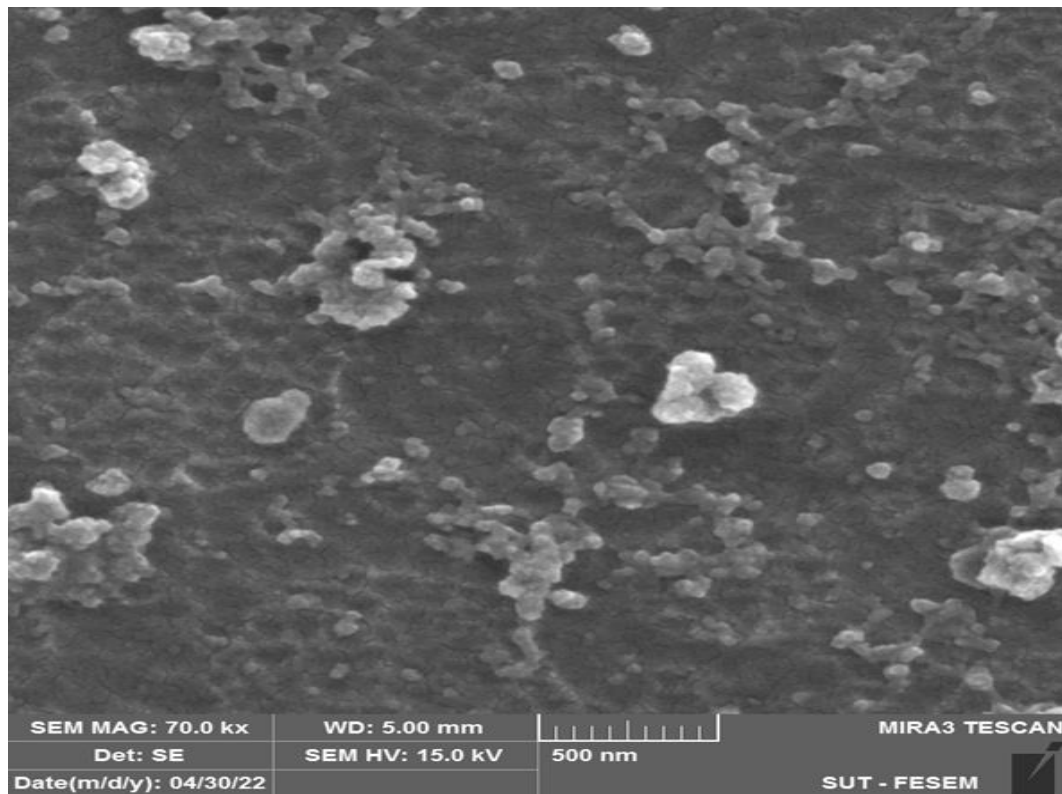


Figure (3-8) SEM Image of Ps layer with HNO_3 +HF at 25 min.

It is possible to make a description of the reaction between HF acid and Ethanol solution with different Etching time for 5 minutes about porous silicon formation in the middle of the area in the sample by using figure (3-9). The reaction between acid and silicon may be stronger than the ends area of sample due to the difference in the loss of chemical charges in the two regions. Additionally, the interaction with the ends became stronger than the center region, which remained columns because the reaction was slow [101]. Over time, the layer is formed and goes. At 15 min " figure(3-10)" one can see Ps formation and some cracks , It occurred as a result of the union of air pore in Ps and the formation of cracks. In a period of 25 minutes, as can be seen, the porous silicon layer will begin to form more clearly, Nanowalls and a sponge-like structure. This image, which is labeled "figure (3-11)" is a particularly good illustration of the nano crystalline silicon [13].

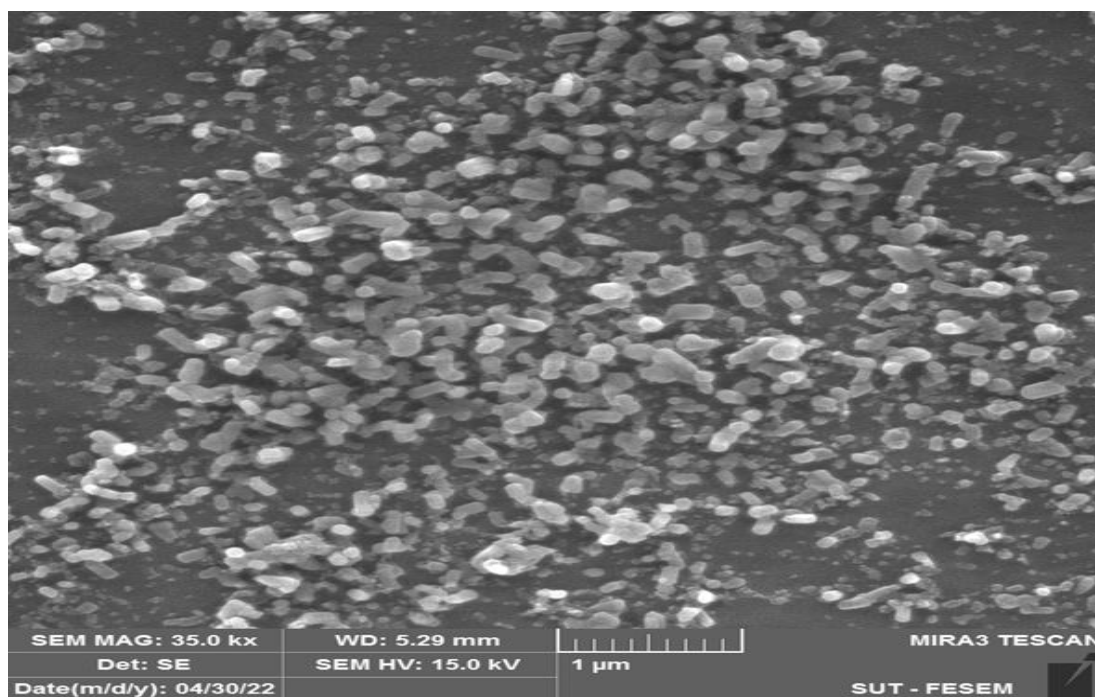


Figure (3-9) SEM of Ps layer in HF+ Ethanol at 5 min

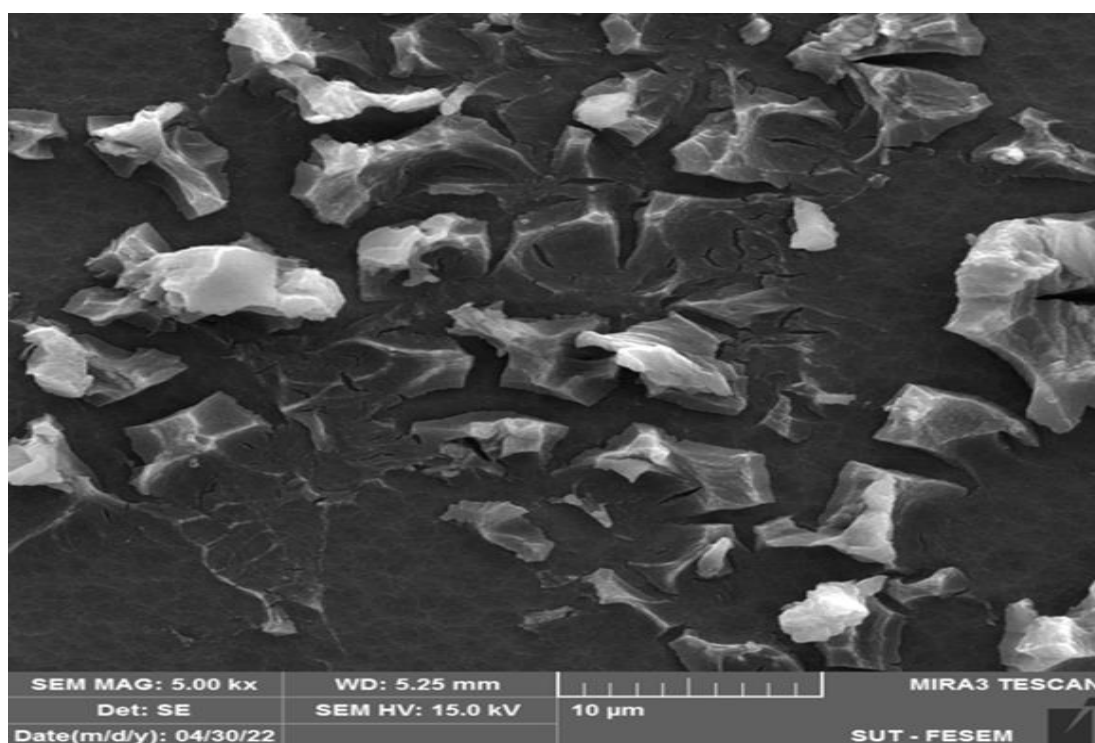


Figure (3-10) SEM of Ps layer in HF + Ethanol at 15 min.

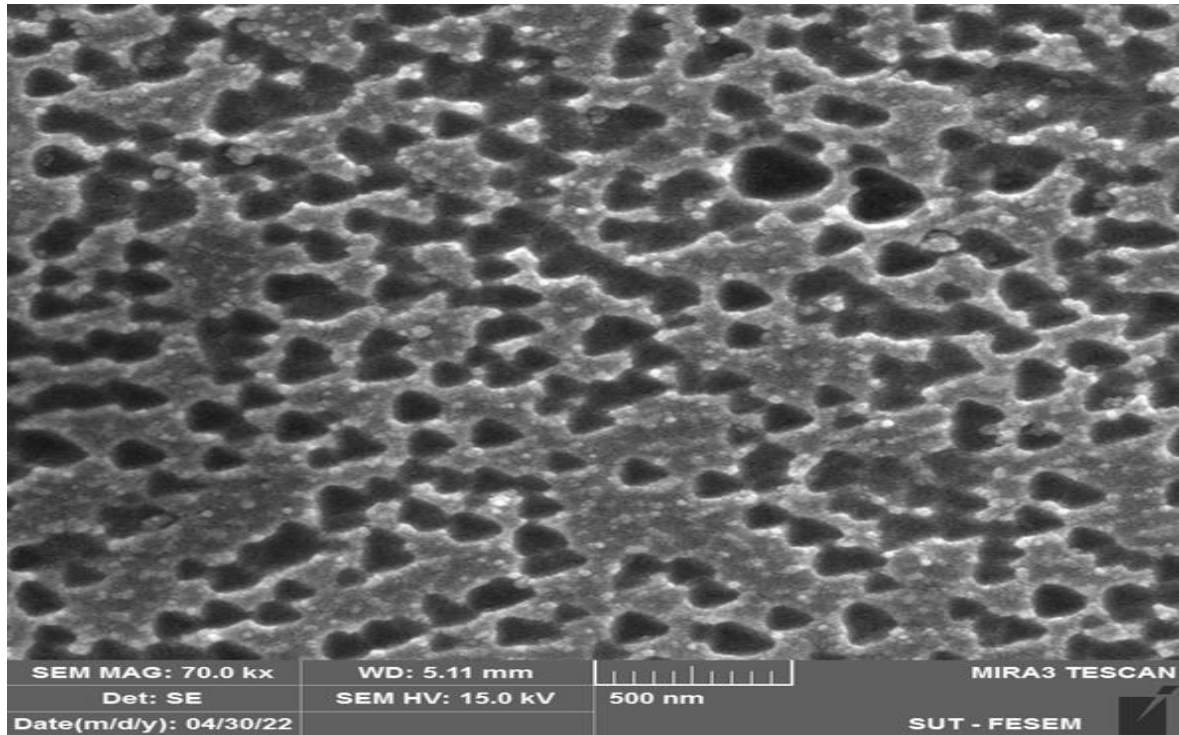


Figure (3-11) SEM of Ps Layer in HF + Ethanol at 25 min.

Nitric acid and salt solution is third solution used in this project ; The creation of the porous layer and nanowalls can be seen, as pointed out , using the SEM images at 15 min, and the nanoscale of this sample can be seen in Figure (3-12).

After a period of time, the reaction proceeds with the development of the porous layer and polishing operations, as shown in figure (3-13) at 20 min, where the polishing of the porous layer is completed, and as a result [102].

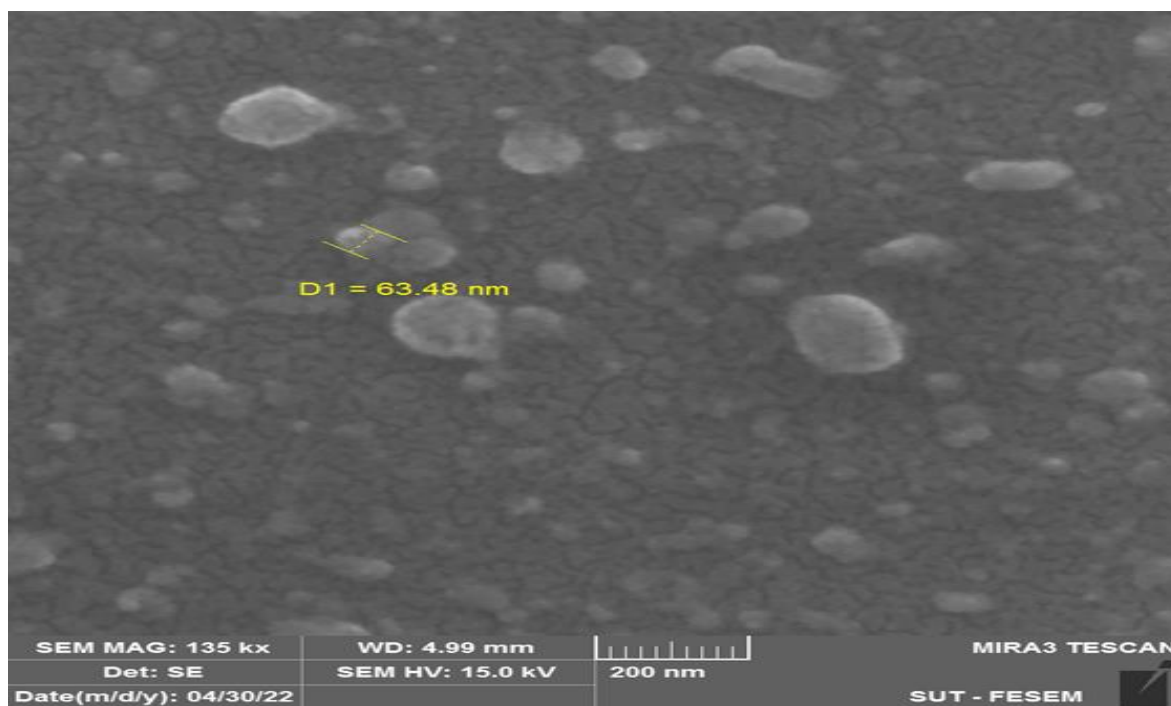


Figure (3-12) SEM of Ps layer in Nitric acid + Salt at 15 min.

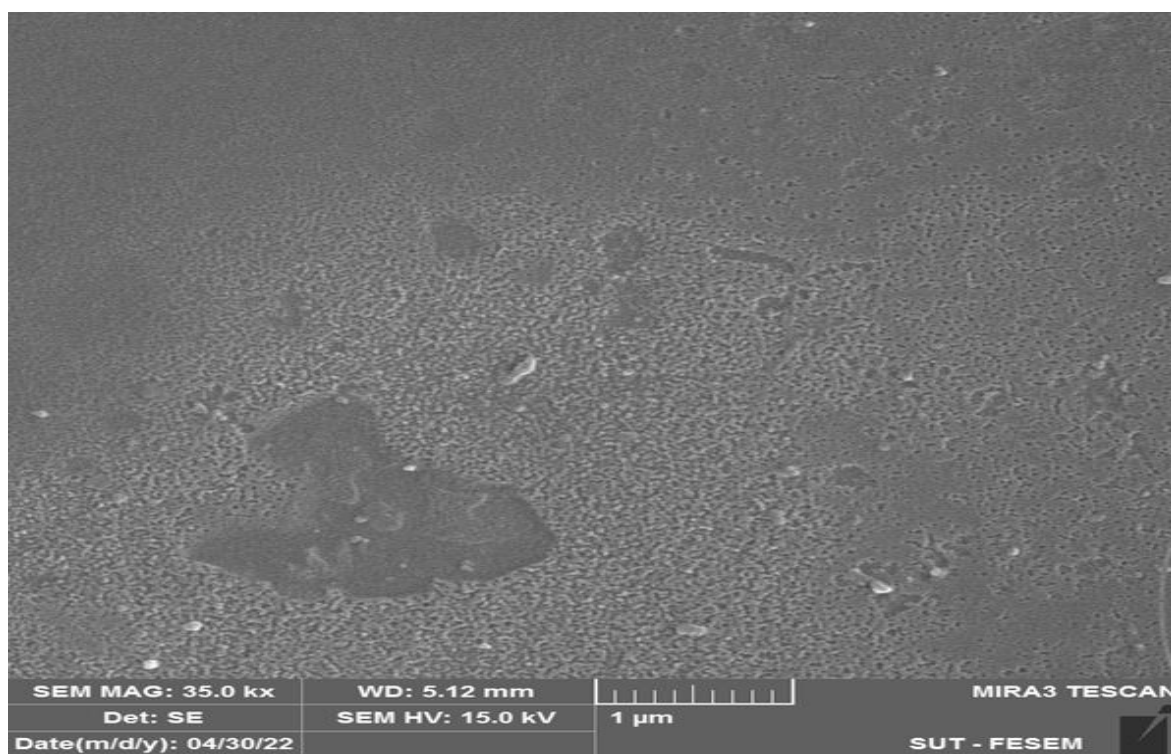


Figure (3-13) SEM of Ps layer in Nitric acid + Salt at 20 min.

Below is a table that includes the values of the nanoscale dimensions of the pores of each sample of acids. One can note through Table (3-1) that the difference in the measurement of the nanoscale dimensions of the pores during different times of HF + Ethanol acid is more uniform and its nano properties are clearer because the smaller the pores, the clearer the nanoscale characteristics.

Table (3-1) Nanoscale of crystalline nano silicon for Samples.

Etching Time (min)	Nanoscale of crystalline nano silicon for Ethanol with HF Samples (nm)	Nanoscale of crystalline nano silicon for Nitric acid with HF Samples (nm)
5	30.40	50.40
10	33.03	49.61
15	32.80	75.05
20	38.26	50.76
25	33.73	39.99
30	40.22	91.85

3.3. Optical Properties

There have been studies done on two different kinds of optical measurements: The relative permittivity and the refractive index. Both of these are closely connected to electrical qualities and the definitions for both may be found in the section that follows.

3.3.a. Relative Permittivity and Refractive Index

There are related to one another because both Refractive index and relative permittivity which factors to morphological features, particularly porosity.

The relative permittivity of Ps may be determined with the help of equation (1-3), whereas the refractive index can be determined with the assistance of equation (1-4).

By noting in figures (3-14) and (3-15) that the values of Refractive index for Nitric acid solution with HF are lower than the results of ethanol solution with HF, the pores of the samples resulting from the reaction of nitric acid with hydrofluoric acid were larger - as previously explained - and this indicates that Silicon material is less, meaning that the air-silicon mixture produced from nitric solution with acid is greater than what is present in samples of ethanol and acid. Consequently, the refractive index created by porous silicon and air is greater in ethanol samples due to the fact that nano silicon has fewer holes and air is less, thus silicon is more abundant [103]. The index of refraction will be greater, reaching the bulk silicon value of 3.5. It may be determined that nitric and hydrofluoric acid contain more silicon than ethanol with the acid [104]. In general these figures are a decreasing in values of refractive index because of the mixture between two matters the refractive index of air and refractive index of silicon [105], but the comparison between them is the ratio between the two matters.

In figure(4-16), a comparison of the values can be noticed.

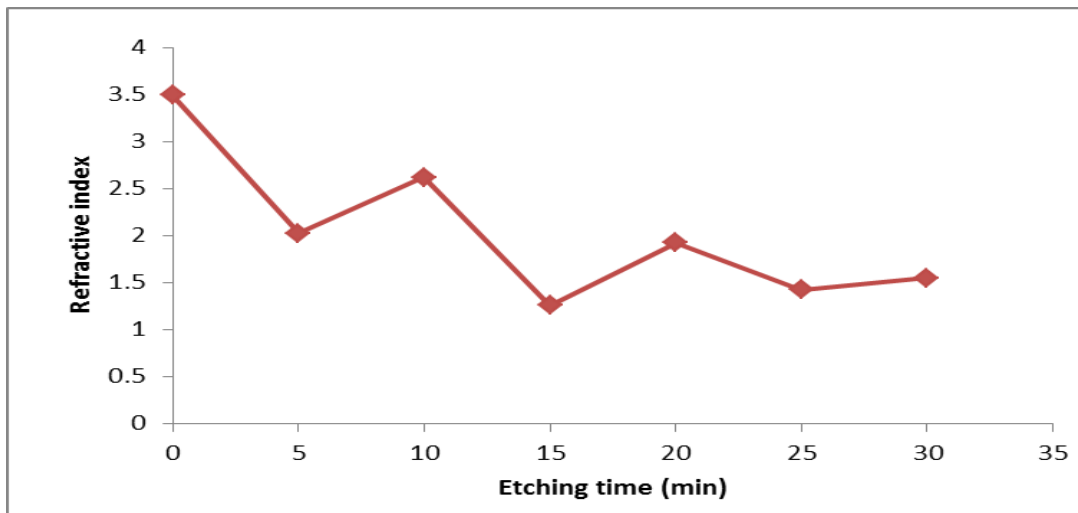


Figure (3-14) Relation between Refractive Index and Time for Nitric acid with HF.

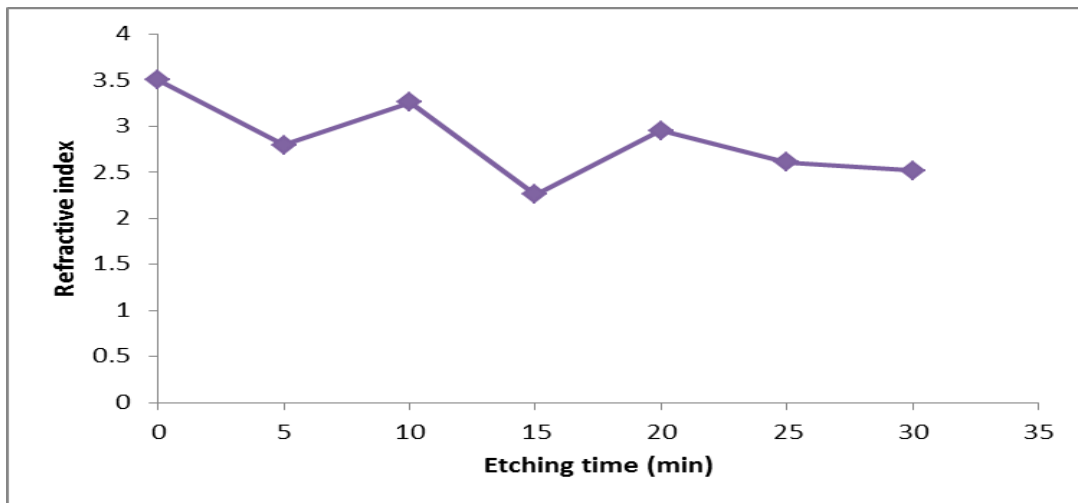


Figure (3-15) Relation between Refractive Index and Time for Ethanol with HF.

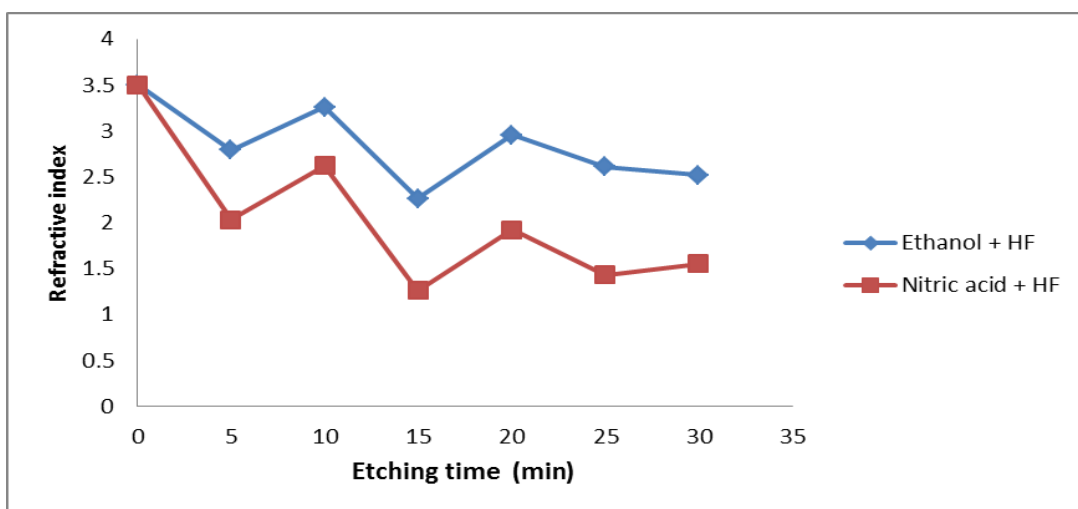


Figure (4-16) Relation between Refractive Index and Time for both solutions.

Also, as shown in Figures (3-17) and (3-18), the relative permittivity values of samples of nitric solution with HF are lower [106], and a dissolution can be seen. Over time, these values move away from the value of bulk silicon, which is 12 [107]; they move closer to the value of air, which is 1, which means there is more air than silicon and the pores are bigger. The pores in the samples of nitric solution are bigger than the pores in the samples of ethanol solution (the holes in Ethanol are small), so the application used with Nitric solution in this stage and time is very specific because the nano walls are very thin [108].

Moreover, figure (3-19), illustrates how the different values of the two solutions compare to each other. This difference is caused by the difference in how the materials interact with each other and by the difference in porosity and how it is mathematically linked to the optical properties.

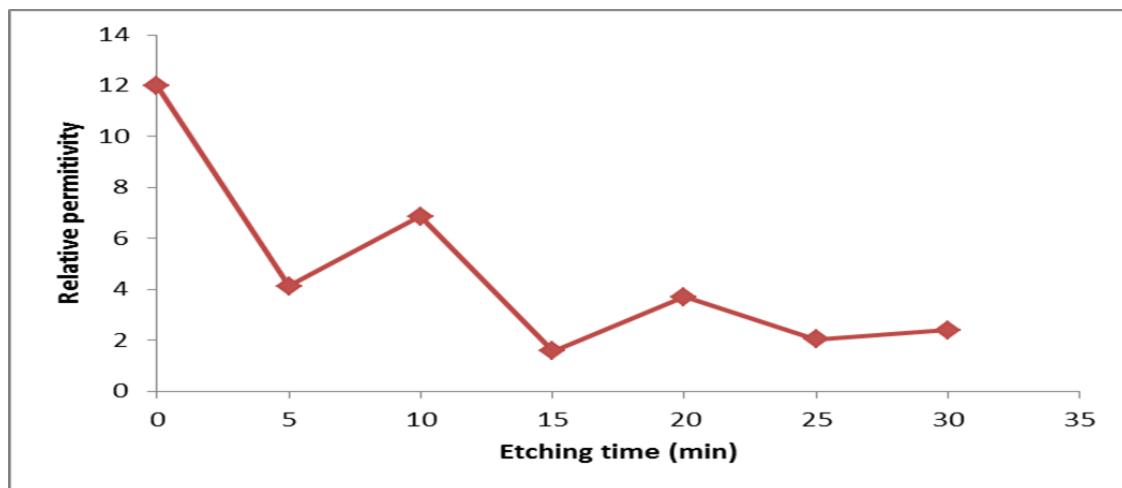


Figure (3-17) Relation between Relative permittivity and time for Nitric acid and HF.

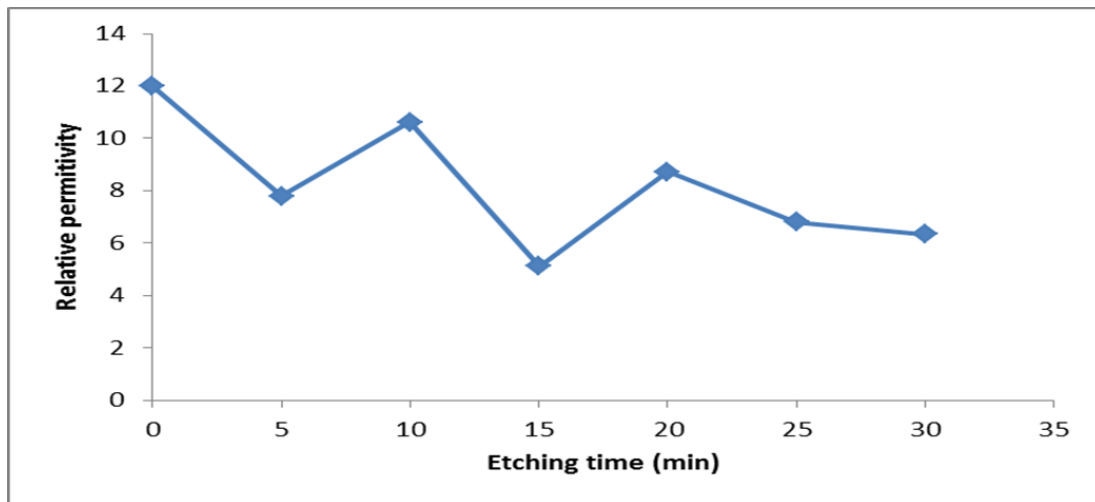


Figure (3-18) Relation between Relative Permittivity and Time for Ethanol with HF.

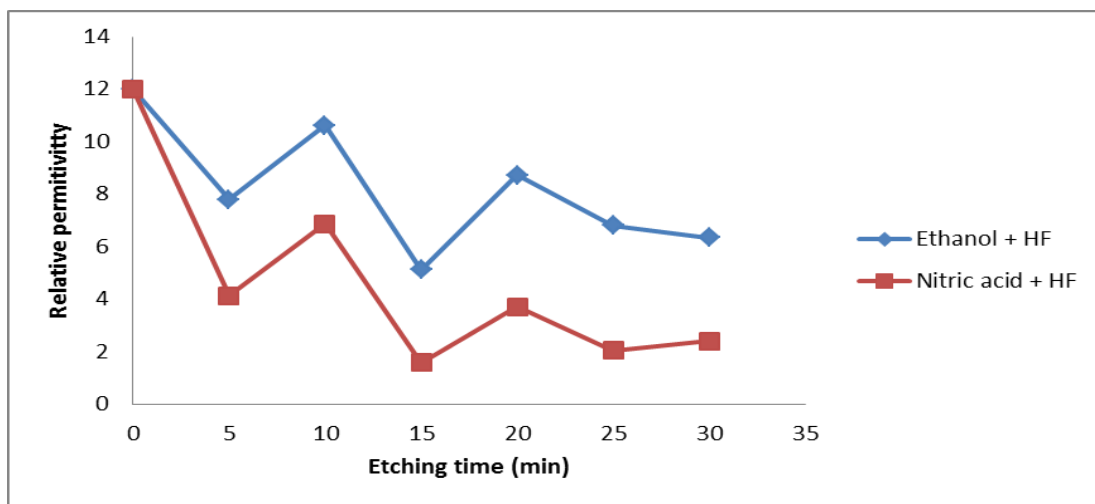


Figure (3-19) Relation between Relative Permittivity and Time for both solutions.

3.4. The Electrical Capacitance for Ps Layer

The capacitance-voltage characteristics of Ps/c-Si structures are influenced in many ways by the shape and porosity of the etched silicon surface

Because the morphological qualities are mathematically connected to one another, the electrical capacitance rises as the relative permittivity rises, and as layer thickness is reduced, the porous layer becomes thinner, the porosity decreases, and the electrical capacitance rises [109].

The most key reason is that capacitance is the opposite of porosity because it depends on the amount of material present (more material = more capacitance), which stores electric charges. When the nano-silicon layer is formed, it turns into holes and the containment of electric charges decreases, which causes the capacitance to decrease [110].

Therefore, the capacity in samples of ethanol solution appeared much higher than that of nitric, and as can be observed in figures (4-20) ,(3-21).

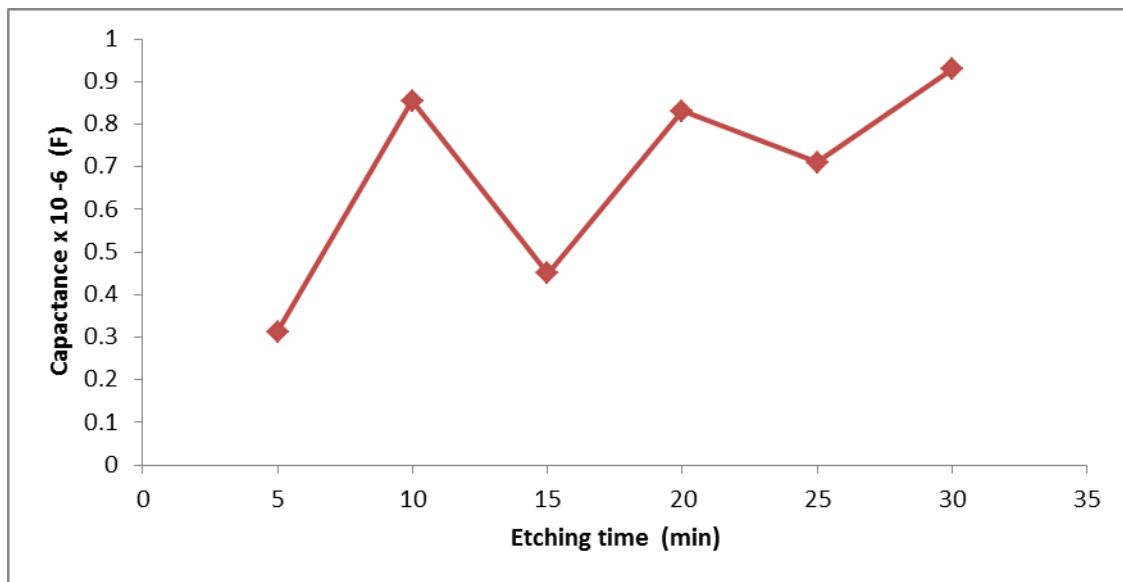


Figure (3-20) Relation between capacitance and Etching time of Nitric acid +HF.

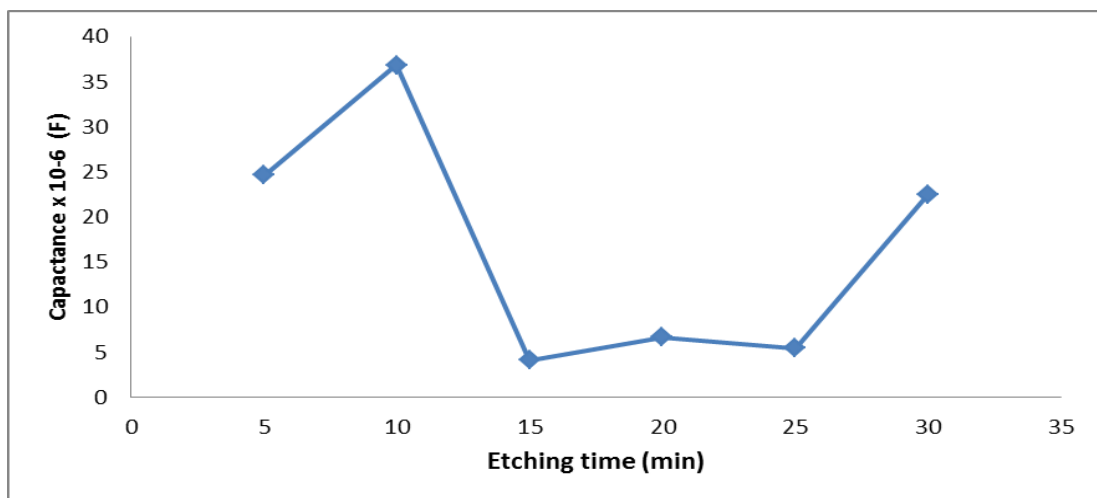


Figure (3-21) Relation between Capacitance and Etching Time of Ethanol + HF.

It is possible to notice the big and clear difference between the results in figure (3-22).

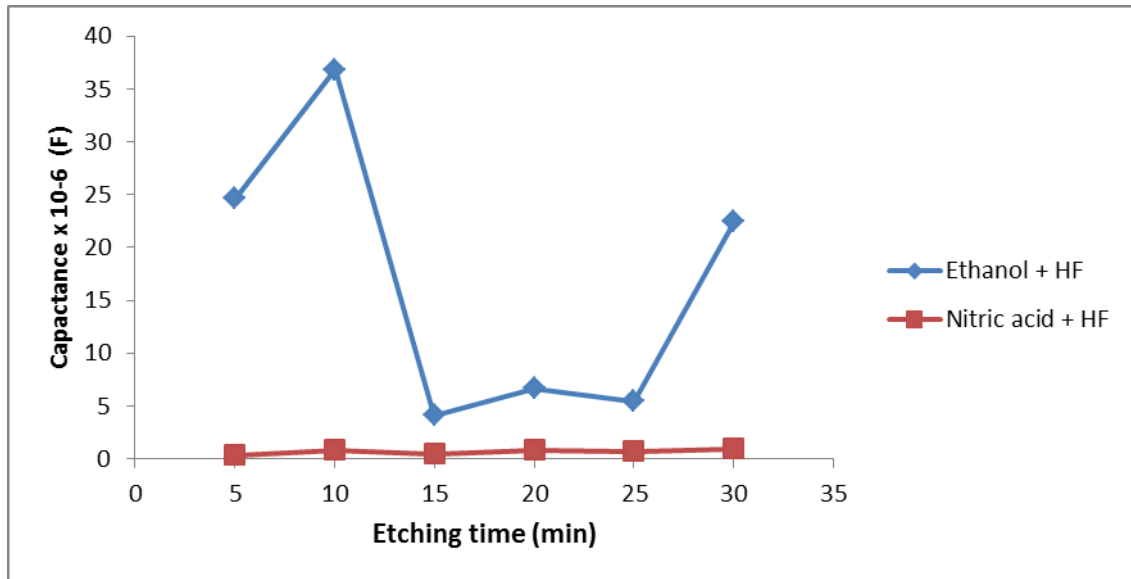
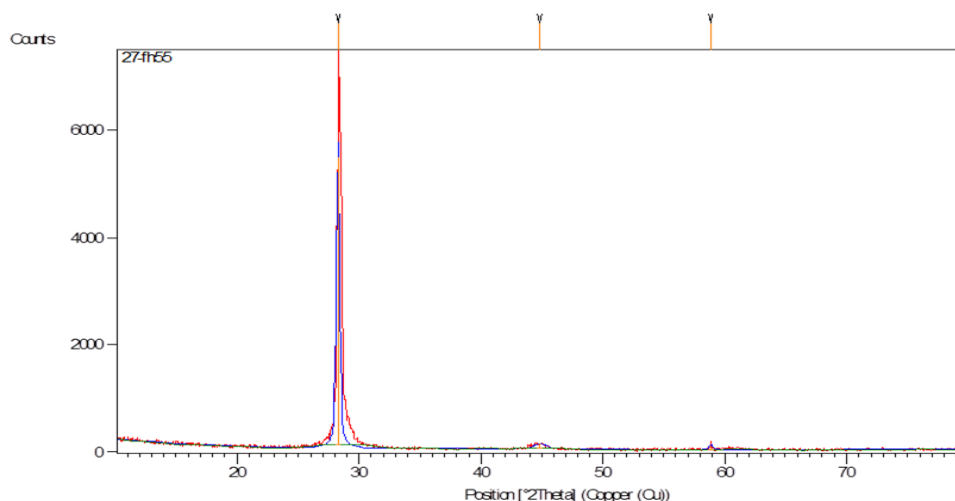


Figure (3-22) Relation between Capacitance and Etching Time of both solutions.

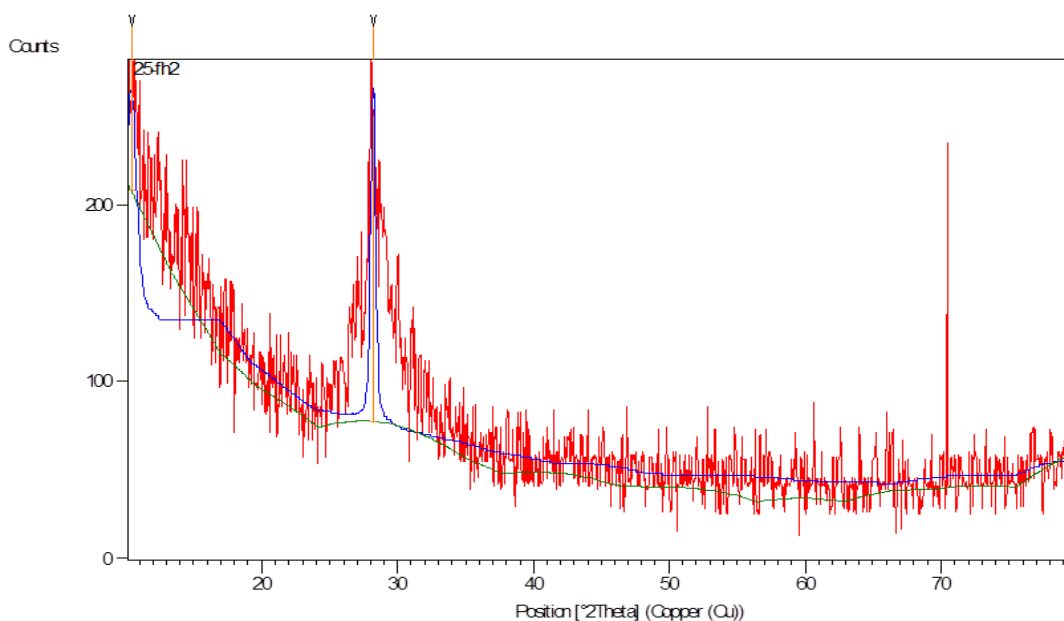
3.5. Porous Silicon's X-Ray Characteristics

In addition to determining silicon nano sizes Ps, the X-ray diffraction test provides insightful information about the morphological characteristics of Ps is a function. A good understanding of the material's electrical and morphological behavior will be provided by the Ps layer's morphological step (crystalline or amorphous) [111].

The X-ray Diffraction for Nitric acid and salt (NaCl) solution in figure (3-23), From this figure, the porous silicon signal can be observed very clearly, and that was at 15 minutes which is out any suspicion one pattern of diffraction with nanoscale .As for the 20 minutes, the formation of a new porous layer started after removing the formed layer at 15 minutes, So this shape close to the bulk silicon because a new etching process is taking place at this moment [112], one can notice this in figure (3-24).



Figure(3-23) X-Ray Diffraction of Ps in HNO₃+SALT at 15 min .



Figure(3-24) X-Ray Diffraction of Ps in HNO₃+SALT at 20 min.

X-ray diffraction for HF + Ethanol at 15 min in figure (3-25) from this figure one can see appeared to be close to bulk silicon as time progressed, the porous layer did indeed form. It is plain to see that the porous layers are developing, and at the same time, nanowalls are coming into being, at 20 min in figure (3-26), one can see the unified model of clear nano silicon [113].

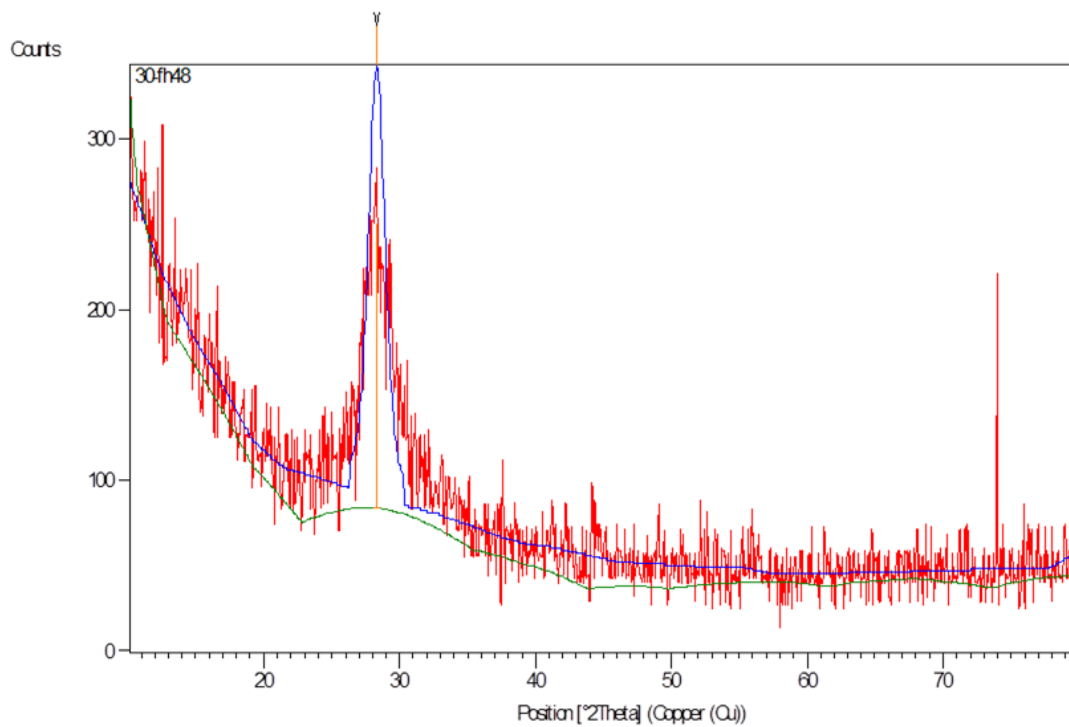


Figure (3-25) X-Ray Diffraction of Ps in HF+Ethanol at 15 min.

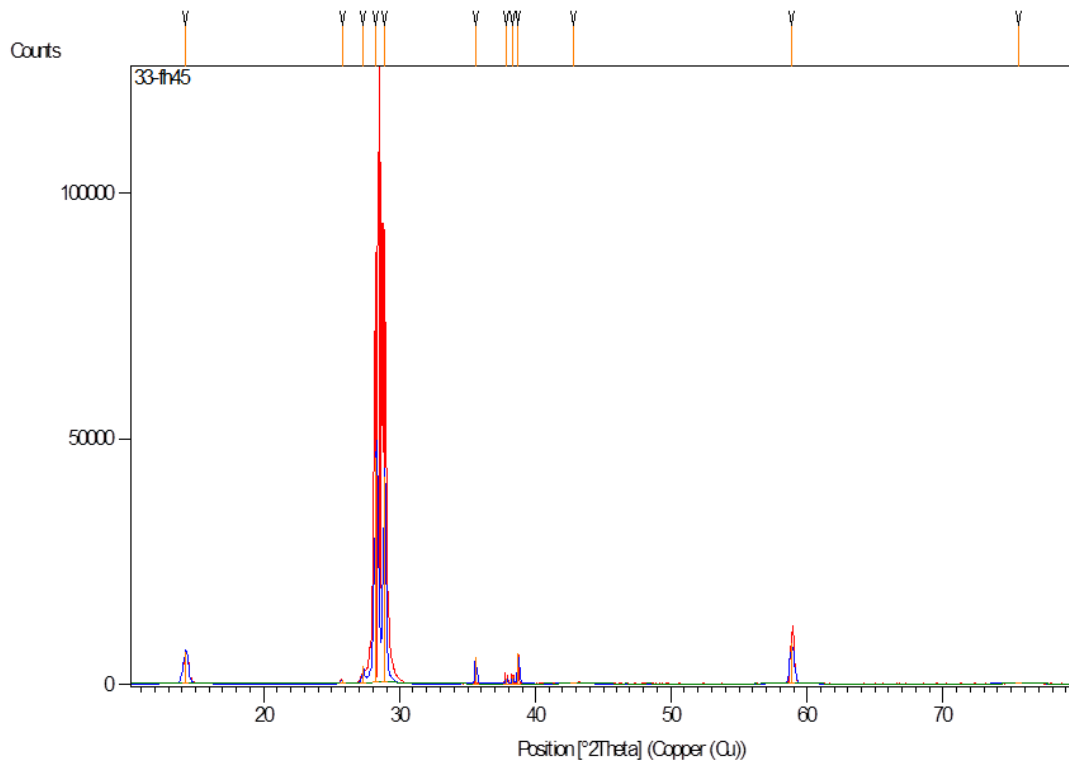
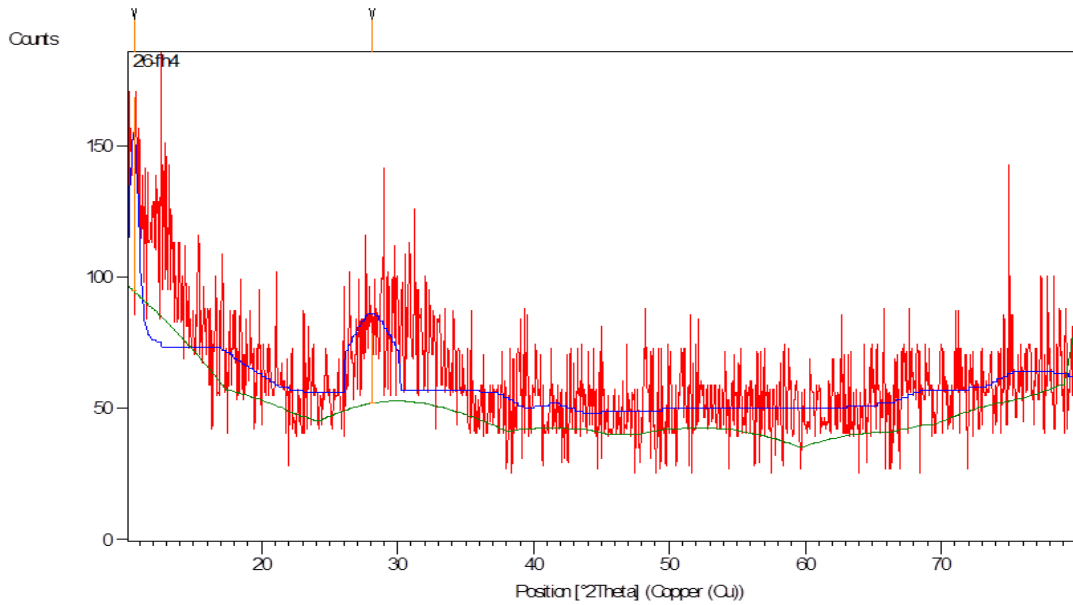
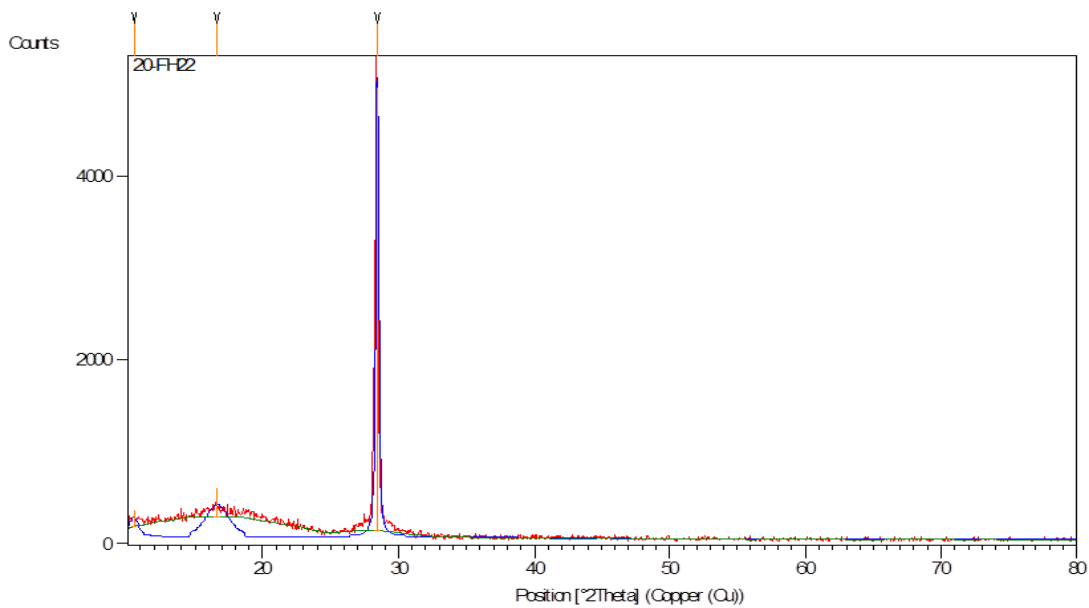


Figure (3-26) X-Ray Diffraction of Ps in HF + Ethanol at 20 min.

The X-Ray Diffraction for samples which prepared in Nitric acid and HF solution, Figure (3-27) appeared multi patterns of nano silicon . However, [114]. It is possible to notice the appearance of the porous silicon layer in the unified model of nano silicon in figure (3-28).



Figure(3-27) X-Ray Diffraction of HNO₃+HF at 5 min .



Figure(3-28) X-Ray Diffraction of HNO₃+HF at 25 min.

Chapter Four

Conclusions and Recommendations

4.1. Conclusions

Considering these results and data,, the method of electro-chemical etching might be considered a highly valuable technology for manufacturing materials with acceptable qualities for usage in a range of applications. This is because Ps materials can be produced by this technique. The following is an overview of the important findings:

1- Electro-chemical etching of silicon, one of the etching processes that are now available which is currently the subject of research. Its characteristics combine those of electro-chemical etching with those of using induced etching to supply an etching procedure that is straightforward, inexpensive, and easy to manage. As a direct consequence, this method may be utilized to etch silicon in a comparatively brief amount of time.

2- The morphological qualities of the Ps that were formed by the approach of electrochemical etching were astounding and very sensitive to the preparation settings, in addition to the perilous nature of the acids that were utilized.

A- The porous silicon layer was grown to have holes, wider pores, and a thicker layer in the presence of Nitric acid with HF solution more than other solutions.

B- Both the thickness of the walls that separate the pores and the size of the nanocrystals were larger in the samples that included ethanol and acid.

C: The manifestation of pores in a variety of forms, including rectangular and cylindrical.

2- When compared to other methods, the amount of time needed to manufacture porous silicon surfaces via electrochemical etching is significantly shorter.

3- The rise and fall of porosity is caused by the relative permittivity and refractive index, which are mathematically linked to the qualities. The relative permittivity and refractive index will go down as porosity goes up.

4- Our data results in the conclusion that one morphological property is connected to another, and that the increase and reduction of one morphological property is mathematically related to the other.

5- The solutions utilized yielded nano silicon. The nano silicon created from nitric acid and HF acid is of good quality, but its pattern is particular, which means that nanosilicon uses for this solution are limited

6- The Nitric + HF reaction is slower than the HF + ethanol reaction.

7- The nanowalls of nano silicon made from ethanol and HF are thicker.

8- When the nano-silicon layer is formed, it turns into holes and the containment of electric charges decreases, which causes the capacitance to decrease in Nitric acid + HF.

4.2. Recommendations

In the future, it would be vital and fascinating to do the following studies:

- 1- Examining the impact of skimming time on structural qualities and identify electrical parameters having a similar impact.
- 2- Studying of the change of negativity of other acids on the optical characteristics of porous silicon
- 3- Studying the properties of porous silicon and their relationship with optical energy density
- 4- Formation of the optical sensor device by porous silicon
- 5-Formation of a solar cell using porous silicon with changing the distance of the electrodes
- 6- Using two systems to produce porous silicon or nano-silicon
- 7- Examining the electrical characteristics of resistivity, compute voltage and current in the dark regions.
- 8- Applying Models in Mathematics to determine the structural features and preparatory conditions.
- 9- Examining the impact of structural characteristics on solar cell performance.

References

References

- [1] A. Mandrikas, E. Michailidi, and D. Stavrou, “Teaching nanotechnology in primary education,” *Res. Sci. Technol. Educ.*, vol. 38, no. 4, pp. 377–395, 2020.
- [2] G. Wang, “Nanotechnology: The new features,” *arXiv Prepr. arXiv1812.04939*, 2018.
- [3] M. F. Mady and M. A. Kelland, “Review of nanotechnology impacts on oilfield scale management,” *ACS Appl. Nano Mater.*, vol. 3, no. 8, pp. 7343–7364, 2020.
- [4] S. Rai and A. Rai, “Nanotechnology-The secret of fifth industrial revolution and the future of next generation,” *J. Nas.*, vol. 7, no. 2, pp. 61–66, 2017.
- [5] K. A. Brown, S. Brittman, N. Maccaferri, D. Jariwala, and U. Celano, “Machine learning in nanoscience: big data at small scales,” *Nano Lett.*, vol. 20, no. 1, pp. 2–10, 2019.
- [6] D. Benedikovic, Daniel Viot, Léopold Aubin, Guy Hartmann, Jean Michel Amar, Farah Le Roux, Xavier Alonso-Ramos, Carlos Cassan, Éric Marris-Morini, Delphin Fédéli, Jean-Marc, “Silicon–germanium receivers for short-wave-infrared optoelectronics and communications,” *Nanophotonics*, vol. 10, no. 3, pp. 1059–1079, 2021.
- [7] R. J. Martín-Palma and J. Martínez-Duart, *Nanotechnology for microelectronics and photonics*. Elsevier, 2017.
- [8] M. Tang, Mingchu Park, Jae-Seong Wang, Zhechao Chen, Siming Jurczak, Pamela Seeds, Alwyn Liu, Huiyun, “Integration of III-V lasers on Si for Si photonics,” *Prog. Quantum Electron.*, vol. 66, pp. 1–18, 2019.
- [9] W. K. Alaarage, L. H. A. Oneiza, and M. G. M. Alzubaidi, “Study of the electrical properties of porous silicon prepared by

References

- electrochemical etching technique,” *J. Southwest Jiaotong Univ.*, vol. 54, no. 5, 2019.
- [10] G. Korotcenkov, *Porous silicon: from formation to application: formation and properties, Volume One*. CRC Press, 2016.
- [11] R. Wu, Rihan Jin, Qihao Storey, Catherine Collins, Jack Gomard, Guillaume Lemmer, Uli Canham, Leigh Kling, Rainer Kaplan, Andrey, “Gold nanoplasmonic particles in tunable porous silicon 3D scaffolds for ultra-low concentration detection by SERS,” *Nanoscale horizons*, vol. 6, no. 10, pp. 781–790, 2021.
- [12] Q. Rong, W. Lei, and M. Liu, “Conductive hydrogels as smart materials for flexible electronic devices,” *Chem. Eur. J.*, vol. 24, no. 64, pp. 16930–16943, 2018.
- [13] N. Burham, A. A. Hamzah, and B. Y. Majlis, “Effect of hydrofluoric acid (HF) concentration to pores size diameter of silicon membrane,” *Biomed. Mater. Eng.*, vol. 24, no. 6, pp. 2203–2209, 2014.
- [14] S. Praveenkumar, D. Lingaraja, P. M. Mathi, and G. D. Ram, “An experimental study of optoelectronic properties of porous silicon for solar cell application,” *Optik (Stuttg.)*, vol. 178, pp. 216–223, 2019.
- [15] F. A. Harraz, “Porous silicon chemical sensors and biosensors: A review,” *Sensors Actuators B Chem.*, vol. 202, pp. 897–912, 2014.
- [16] R. A. Perez and G. Mestres, “Role of pore size and morphology in musculo-skeletal tissue regeneration,” *Mater. Sci. Eng. C*, vol. 61, pp. 922–939, 2016.
- [17] F. Iacona, Fabio Irrera, Alessia Franzo, Giorgia Pacifici, Domenico Crupi, Isodiana Miritello, Maria Presti, Calogero D

- Priolo, Francesco, “Silicon-based light-emitting devices: properties and applications of crystalline, amorphous and Er-doped nanoclusters,” *IEEE J. Sel. Top. Quantum Electron.*, vol. 12, no. 6, pp. 1596–1606, 2006.
- [18] S. Trolier-McKinstry and R. E. Newnham, *Materials engineering: bonding, structure, and structure-property relationships*. Cambridge University Press, 2018.
- [19] C. Kamaraki, M. T. Klug, T. Green, L. Miranda Perez, and C. Case, “Perovskite/silicon tandem photovoltaics: Technological disruption without business disruption,” *Appl. Phys. Lett.*, vol. 119, no. 7, p. 70501, 2021.
- [20] D. R. Huanca, “Porous Silicon: A Sponge-Like Structure for Photonic Based Sensor Devices,” in *21st Century Nanoscience—A Handbook*, CRC Press, pp. 1–4, 2020.
- [21] F. V Antolinez, F. T. Rabouw, A. A. Rossinelli, J. Cui, and D. J. Norris, “Observation of electron shakeup in CdSe/CdS core/shell nanoplatelets,” *Nano Lett.*, vol. 19, no. 12, pp. 8495–8502, 2019.
- [22] R. Wu *et al.*, “Taming non-radiative recombination in Si nanocrystals interlinked in a porous network,” *Phys. Chem. Chem. Phys.*, 2022.
- [23] R. Moretta, L. De Stefano, M. Terracciano, and I. Rea, “Porous silicon optical devices: recent advances in biosensing applications,” *Sensors*, vol. 21, no. 4, p. 1336, 2021.
- [24] P. Granitzer and K. Rumpf, “Porous silicon—a versatile host material,” *Materials (Basel)*, vol. 3, no. 2, pp. 943–998, 2010.

References

- [25] Y. Liu, L. Qin, F. Liu, Y. Fan, J. Ruan, and S. Zhang, “Interpenetrated 3D porous silicon as high stable anode material for Li-Ion battery,” *J. Power Sources*, vol. 406, pp. 167–175, 2018.
- [26] P. Elia, E. Nativ-Roth, Y. Zeiri, and Z. Porat, “Determination of the average pore-size and total porosity in porous silicon layers by image processing of SEM micrographs,” *Microporous Mesoporous Mater.*, vol. 225, pp. 465–471, 2016.
- [27] D. A. Eurov *et al.*, “Cobalt oxide decorated porous silica particles: Structure and activity relationship in the catalytic oxidation of carbon monoxide,” *Appl. Surf. Sci.*, vol. 579, p. 152121, 2022.
- [28] I. A. Abbas and S. Q. Hazaa, “Study the Effect of Etching Time on the Characteristics of the Porous Silicon that Prepare from N-Type Silicon by Photoelectrochemical Etching Method, vol. 23, no. 2, 2022.
- [29] H.-C. Huang, Z. Ren, C. Chan, and X. Li, “Wet etch, dry etch, and MacEtch of β -Ga₂O₃: A review of characteristics and mechanism,” *J. Mater. Res.*, pp. 1–15, 2021.
- [30] V. Lotito and T. Zambelli, “Playing with sizes and shapes of colloidal particles via dry etching methods,” *Adv. Colloid Interface Sci.*, vol. 299, p. 102538, 2022.
- [31] S. Kalem and O. Yavuzcetin, “Possibility of fabricating light-emitting porous silicon from gas phase etchants,” *Opt. Express*, vol. 6, no. 1, pp. 7–11, 2000.
- [32] O. M. Zhigalina, D. N. Khmelenin, A. V Atanova, N. V Minaev, A. P. Sviridov, and M. Y. Tsvetkov, “A nanoscale modification of materials at thermoplasmonic laser-induced backside wet etching of

- sapphire,” *Plasmonics*, vol. 15, no. 3, pp. 599–608, 2020.
- [33] X. Yang, Fengshuo Chen, Xiuhua Li, Shaoyuan Wan, Xiaohan Ma, Wenhui Dong, Peng Duan, Jianguo Chang, Yuanchih, “Porous Silicon Fabrication and Surface Cracking Behavior Research Based on Anodic Electrochemical Etching,” *Fuel Cells*, vol. 21, no. 1, pp. 52–57, 2021.
- [34] M. Brinker, Guido Richert, Claudia Lakner, Pirmin Krekeler, Tobias Keller, Thomas F Huber, Norbert Huber, Patrick., “Giant electrochemical actuation in a nanoporous silicon-polypyrrole hybrid material,” *Sci. Adv.*, vol. 6, no. 40, p. eaba1483, 2020.
- [35] M. C. Arenas, M. Vega, O. Martínez, and O. H. Salinas, “Nanocrystalline porous silicon: structural, optical, electrical and photovoltaic properties,” *Chapter from B. “Crystalline Silicon–Properties Uses*, pp. 251–274, 2011.
- [36] J. M. Weisse, *Fabrication and characterization of vertical silicon nanowire arrays: A promising building block for thermoelectric devices*. Stanford University, 2013.
- [37] Y. Chao, L. Q. Wu, and X. L. Luo, “Study on Multi-crystalline Silicon Textured by ultrasound,” in *Applied Mechanics and Materials*, vol. 130, pp. 50–53, 2012.
- [38] K. W. Kolasinski and J. Yadlovskiy, “Stain etching of silicon with V₂O₅,” *Phys. Status Solidi*, vol. 8, pp. 1749–1753, 2011.
- [39] H. A. A. Amir, M. A. Fakhri, A. A. Alwahib, E. T. Salim, F. H. Alsultany, and U. Hashim, “An investigation on GaN/Porous-Si NO₂ Gas Sensor fabricated by Pulsed Laser Ablation in Liquid,” *Sensors Actuators B Chem.*, p. 132163, 2022.

- [40] A. Akbıyık, N. Avishan, Ö. Demirtaş, A. K. Demir, E. Yüce, and A. Bek, “Laser Photochemical Nanostructuring of Silicon for Surface Enhanced Raman Spectroscopy,” *Adv. Opt. Mater.*, vol. 10, no. 14, p. 2200114, 2022.
- [41] Q. Wang, “Metal-assisted photochemical etching of GaN nanowires: The role of metal distribution,” *Electrochem. Commun.*, vol. 103, pp. 66–71, 2019.
- [42] S. V ZaboltnovKurakina, D A Kashaev, F V Skobelkina, A V Kolchin, A V Kaminskaya, T P Khilov, A V Agrba, P D Sergeeva, E A Kashkarov, P K Kirillin, M.Yu., “Structural and optical properties of nanoparticles formed by laser ablation of porous silicon in liquids: Perspectives in biophotonics,” *Quantum Electron.*, vol. 50, no. 1, p. 69, 2020, doi: 10.1070/QEL17208.
- [43] M. Van den Bergh, Matthias Krajnc, Andraž Voorspoels, Stefan Tavares, Sergio Rodrigues Mullens, Steven Beurroies, Isabelle Maurin, Guillaume Mali, Gregor De Vos, Dirk E, “Highly Selective Removal of Perfluorinated Contaminants by Adsorption on All-Silica Zeolite Beta,” *Angew. Chemie*, vol. 132, no. 33, pp. 14190–14194, 2020.
- [44] M. F. Fink, M. Weiss, R. Marschall, and C. Roth, “Experimental correlation of Mn 3+ cation defects and electrocatalytic activity of α -MnO₂—an X-ray photoelectron spectroscopy study,” *J. Mater. Chem. A*, vol. 10, no. 29, pp. 15811–15838, 2022.
- [45] N. H. Harb and F. A.-H. Mutlak, “Production and characterization of porous silicon via laser-assisted etching: Effect of gamma irradiation,” *Optik (Stuttg.)*, vol. 246, p. 167800, 2021.

References

- [46] J. SarkarMridha, Deepanjan Sarkar, Joy Orasugh, Jonathan Tersur Gangopadhyay, Bhuman Chattopadhyay, Dipankar Roychowdhury, Tarit Acharya, Krishnendu, “Synthesis of nanosilica from agricultural wastes and its multifaceted applications: A review,” *Biocatal. Agric. Biotechnol.*, vol. 37, p. 102175, 2021.
- [47] P. A. Maughan, “Porous silica-pillared MXenes with controllable interlayer distances for long-life Na-ion batteries,” *Langmuir*, vol. 36, no. 16, pp. 4370–4382, 2020.
- [48] Z. Jiang and B. Lee, “Recent advances in small angle X-ray scattering for superlattice study,” *Appl. Phys. Rev.*, vol. 8, no. 1, p. 11305, 2021.
- [49] S. Pillet, “Spin-crossover materials: Getting the most from x-ray crystallography,” *J. Appl. Phys.*, vol. 129, no. 18, p. 181101, 2021.
- [50] T. Jiang, “Morphology, composition and electrochemistry of a nano-porous silicon versus bulk silicon anode for lithium-ion batteries,” *J. Mater. Sci.*, vol. 52, no. 7, pp. 3670–3677, 2017.
- [51] E. G. Chadwick, S. Beloshapkin, and D. A. Tanner, “Microstructural characterisation of metallurgical grade porous silicon nanosponge particles,” *J. Mater. Sci.*, vol. 47, no. 5, pp. 2396–2404, 2012.
- [52] A. S. Alber and F. A.-H. Mutlak, “The role of various etching time in Si nanostructures for ultra-high sensitivity photodetector,” *Optik (Stuttg.)*, vol. 265, p. 169427, 2022.
- [53] L. SiWei, Jianping Xi, Yujun Wang, Hongyang Wen, Zhihui Li, Bo Zhang, Hongtu, “The influence of long-time water intrusion on the mineral and pore structure of coal,” *Fuel*, vol. 290, p. 119848, 2021.

References

- [54] F. HanZhong, Zhaoxiang Yang, Yi Wei, We Zhang, Feng Xing, Weihong Fan, Yiqun, “High gas permeability of SiC porous ceramics reinforced by mullite fibers,” *J. Eur. Ceram. Soc.*, vol. 36, no. 16, pp. 3909–3917, 2016.
- [55] S. Meng, J. Zhang, W. Chen, X. Wang, and M. Zhu, “Construction of continuous hollow silica aerogel fibers with hierarchical pores and excellent adsorption performance,” *Microporous Mesoporous Mater.*, vol. 273, pp. 294–296, 2019.
- [56] N. M. Kadum, “Study the Properties of Porous Silicon for P-type and N-type Bulk Silicon.” University of Kerbala, 2015.
- [57] A. P. Oksanich, S. E. Pritchins, M. G. Kogdas, A. G. Kholod, and I. V Shevchenko, “Effect of porous GaAs layer morphology on Pd/porous GaAs Schottky contact,” 2019.
- [58] R. Fopase, S. Paramasivam, P. Kale, and B. Paramasivan, “Strategies, challenges and opportunities of enzyme immobilization on porous silicon for biosensing applications,” *J. Environ. Chem. Eng.*, vol. 8, no. 5, p. 104266, 2020.
- [59] J. B. Cook, Hyung-Seok Lin, Terri C Robbennolt, Shauna Detsi, Eric Dunn, Bruce S Tolbert, Sarah H, “Tuning porosity and surface area in mesoporous silicon for application in Li-ion battery electrodes,” *ACS Appl. Mater. Interfaces*, vol. 9, no. 22, pp. 19063–19073, 2017.
- [60] A. A. Shuihab and S. A. Khalf, “Porous silicon: fabrication, characterization and photoelectronic applications,” *World Sci. News*, vol. 97, pp. 264–273, 2018.
- [61] B. Huang, C. H. Bartholomew, and B. F. Woodfield, “Improved

References

- calculations of pore size distribution for relatively large, irregular slit-shaped mesopore structure,” *Microporous mesoporous Mater.*, vol. 184, pp. 112–121, 2014.
- [62] K. X. Wang, Z. Yu, V. Liu, Y. Cui, and S. Fan, “Absorption enhancement in ultrathin crystalline silicon solar cells with antireflection and light-trapping nanocone gratings,” *Nano Lett.*, vol. 12, no. 3, pp. 1616–1619, 2012.
- [63] A. K. Al-Kadumi, “The effect of the etching time on the electrical properties of nano structure silicon,” *Iraqi J. Phys.*, vol. 10, no. 18, pp. 1–4, 2012.
- [64] H. Shim, F. Monticone, and O. D. Miller, “Fundamental limits to the refractive index of transparent optical materials,” *Adv. Mater.*, vol. 33, no. 43, p. 2103946, 2021.
- [65] J. Salonen and E. Mäkilä, “Thermally carbonized porous silicon and its recent applications,” *Adv. Mater.*, vol. 30, no. 24, p. 1703819, 2018.
- [66] A. J. K. U. M. Nayef A.M. Abdul Hussein, “Preparation and Characterization Study of Porous Silicon Doped with Cu and Ag,” *Eng. Technol. J.*, vol. 35, no. 1, pp. 8–12, 2017, [Online]. Available: https://etj.uotechnology.edu.iq/article_133668.html
- [67] N. M. Al-Rahime, H. I. Salman, and A. K. Al-Kadumi, “The effect of the acid concentration on morphology of nano crystalline silicon,” *Mater. Today Proc.*, vol. 45, pp. 5535–5538, 2021.
- [68] R.-A. Mitran, S. Ioniță, D. Lincu, D. Berger, and C. Matei, “A review of composite phase change materials based on porous silica nanomaterials for latent heat storage applications,” *Molecules*, vol.

References

- 26, no. 1, p. 241, 2021.
- [69] N. Naderi and M. Moghaddam, “Ultra-sensitive UV sensors based on porous silicon carbide thin films on silicon substrate,” *Ceram. Int.*, vol. 46, no. 9, pp. 13821–13826, 2020.
- [70] M.-D. Cheng, “Atmospheric chemistry of hydrogen fluoride,” *J. Atmos. Chem.*, vol. 75, no. 1, pp. 1–16, 2018.
- [71] S. Bayne and M. Carlin, *Forensic applications of high performance liquid chromatography*. CRC press, 2017.
- [72] B. L. Fina and A. Rigalli, “The chemistry of fluorine,” *Fluorine; R. Soc. Chem. London, UK*, pp. 41–53, 2015.
- [73] O. A. Al-Owaedi, “Structural, Morphological and Electrical Properties of Porous Silicon Prepared Under Laser Illumination,” *arXiv Prepr. arXiv1612.04865*, 2016.
- [74] G. Korotcenkov, “Porous Silicon Characterization and Application: General View,” in *Porous Silicon: From Formation to Application: Formation and Properties, Volume One*, CRC Press, pp. 20–43, 2016.
- [75] A. M. Mouafki, F. Bouaïcha, A. Hedibi, and A. Gueddim, “Porous Silicon Antireflective Coatings for Silicon Solar Cells,” *Eng. Technol. Appl. Sci. Res.*, vol. 12, no. 2, pp. 8354–8358, 2022.
- [76] W. He, R. Wu, I. V Yurkevich, L. T. Canham, and A. Kaplan, “Reconstructing charge-carrier dynamics in porous silicon membranes from time-resolved interferometric measurements,” *Sci. Rep.*, vol. 8, no. 1, pp. 1–7, 2018.
- [77] M. J. Sailor, *Porous silicon in practice: preparation*,

- characterization and applications*. John Wiley & Sons, 2012.
- [78] B. J. Gelloz, “Luminescent properties of porous silicon,” *Porous Silicon From Form. to Appl. Form. Prop.*, vol. 1, pp. 187–216, 2016.
- [79] S. Basu and J. Kanungo, “Nanocrystalline porous silicon,” in *Crystalline Silicon-Properties and Uses*, IntechOpen, 2011.
- [80] M. P. Stewart and J. M. Buriak, “Chemical and biological applications of porous silicon technology,” *Adv. Mater.*, vol. 12, no. 12, pp. 859–869, 2000.
- [81] P. Dong, G. Hou, X. Xi, R. Shao, and F. Dong, “WO₃-based photocatalysts: morphology control, activity enhancement and multifunctional applications,” *Environ. Sci. Nano*, vol. 4, no. 3, pp. 539–557, 2017.
- [82] L. Yang, Y. Liu, and X. Du, “Advanced Texturing,” *Photovolt. Manuf. Etching, Texturing, Clean.*, pp. 83–113, 2021.
- [83] Z. Nansheng, M. Zhongquan, Z. Chengyue, and H. Bo, “Lower reflectivity and higher minority carrier lifetime of hand-tailored porous silicon,” *J. Semicond.*, vol. 30, no. 7, p. 72004, 2009.
- [84] R. F. Sierra-Moreno, I. A. Lujan-Cabrera, J. M. Cabrera-Teran, E. Ortiz-Vazquez, M. E. Rodriguez-Garcia, and C. F. Ramirez-Gutierrez, “Study of the optical response of oxidized porous silicon structures by thermal oxidation in air,” *J. Mater. Sci.*, vol. 57, no. 24, pp. 11226–11241, 2022.
- [85] R. A. Ismail, N. F. Habubi, and A. N. Abd, “Morphological, Structural and Chemical Properties of p-type Porous Silicon

References

- Produced by Electrochemical Etching,” *Int. J. Thin Film Sci. Technol.*, vol. 3, no. 3, p. 7, 2014.
- [86] L. Zhen-Kun, K. Yi-Lan, C. Hao, and H. Ming, “Variability on Raman shift to stress coefficient of porous silicon,” *Chinese Phys. Lett.*, vol. 23, no. 6, p. 1623, 2006.
- [87] V. Morandi, F. Marabelli, V. Amendola, M. Meneghetti, and D. Comoretto, “Colloidal photonic crystals doped with gold nanoparticles: spectroscopy and optical switching properties,” *Adv. Funct. Mater.*, vol. 17, no. 15, pp. 2779–2786, 2007.
- [88] S. Malarvizhi and V. Balasubramanian, “Influences of tool shoulder diameter to plate thickness ratio (D/T) on stir zone formation and tensile properties of friction stir welded dissimilar joints of AA6061 aluminum–AZ31B magnesium alloys,” *Mater. Des.*, vol. 40, pp. 453–460, 2012.
- [89] S. Mourya, A. Kumar, J. Jaiswal, G. Malik, B. Kumar, and R. Chandra, “Development of Pd-Pt functionalized high performance H₂ gas sensor based on silicon carbide coated porous silicon for extreme environment applications,” *Sensors Actuators B Chem.*, vol. 283, pp. 373–383, 2019.
- [90] V. V Starkov, E. A. Gosteva, D. M. Sedlovets, and M. O. Kah, “Silicon structures with variable morphology of pores methods of obtaining physical and optical properties,” *J. Electrochem. Soc.*, vol. 165, no. 11, p. E534, 2018.
- [91] U. Saha, *Control of Pore Characteristics of Porous Silicon Using Nontoxic Electrochemical Etching for Photovoltaics and Supercapacitor Applications*. South Dakota State University, 2017.

- [92] S. Lin, Y. Fu, Y. Sang, Y. Li, B. Li, and Y. Yang, “Characterization of chiral carbonaceous nanotubes prepared from four coiled tubular 4, 4'-biphenylene-silica nanoribbons,” *AIMS Mater. Sci.*, vol. 1, no. 1, pp. 1–10, 2014.
- [93] H. GuLi, Geping Liu, Chengze Yuan, Fusen Zhang, Lifeng, “Characterization of the products obtained from the reactions of Zircaloy-4 with an acid mixture of concentrated HNO₃ and dilute HF with the aim of understanding pickle salts of zirconium alloys,” *RSC Adv.*, vol. 6, no. 111, pp. 109815–109825, 2016.
- [94] R. Vercauteren, G. Scheen, J.-P. Raskin, and L. A. Francis, “Porous silicon membranes and their applications: Recent advances,” *Sensors Actuators A Phys.*, vol. 318, p. 112486, 2021.
- [95] R. F. Balderas-Valadez, V. Agarwal, and C. Pacholski, “Fabrication of porous silicon-based optical sensors using metal-assisted chemical etching,” *RSC Adv.*, vol. 6, no. 26, pp. 21430–21434, 2016.
- [96] A. Shokrollahi, M. Zare, and F. E. Seraji, “Synthesis and Characterization of p Porous Silicon Layers for Optical Waveguide Applications,” *Environ. Sci.*, vol. 8, p. 9, 2011.
- [97] D. Wu, F. Xu, B. Sun, R. Fu, H. He, and K. Matyjaszewski, “Design and preparation of porous polymers,” *Chem. Rev.*, vol. 112, no. 7, pp. 3959–4015, 2012.
- [98] W. Liu, Zehua Fontana, Flavia Ding, Yaping Liu, Dongfei, “Tailoring porous silicon for biomedical applications: from drug delivery to cancer immunotherapy,” *Adv. Mater.*, vol. 30, no. 24, p. 1703740, 2018.

- [99] Li, Yangyang Zhu, Huilong Kong, Zhenzhen Zhang, Yongkui, “The effect of doping on the digital etching of silicon-selective silicon–germanium using nitric acids,” *Nanomaterials*, vol. 11, no. 5, p. 1209, 2021.
- [100] L. Wu, P. Zhang, C. Feng, J. Gao, B. Yu, and L. Qian, “Scanning probe-based nanolithography: nondestructive structures fabricated on silicon surface via distinctive anisotropic etching in HF/HNO₃ mixtures,” *J. Mater. Sci.*, vol. 56, no. 5, pp. 3887–3899, 2021.
- [101] Y. H. Guan *et al.*, “A hydrofluoric acid-free synthesis of 2D vanadium carbide (V₂C) MXene for supercapacitor electrodes,” *2D Mater.*, vol. 7, no. 2, p. 25010, 2020.
- [102] N. D. Shcherban, “Review on synthesis, structure, physical and chemical properties and functional characteristics of porous silicon carbide,” *J. Ind. Eng. Chem.*, vol. 50, pp. 15–28, 2017.
- [103] R. Bittner, “Liquid-repellent surfaces based on nanostructured silicon substrates.” Wien, 2017.
- [104] Xu, Huajun Liu, Fenggang, “Ultrahigh electro-optic coefficients, high index of refraction, and long-term stability from Diels–Alder cross-linkable binary molecular glasses,” *Chem. Mater.*, vol. 32, no. 4, pp. 1408–1421, 2020.
- [105] D. H. Kim, “One-step vapor-phase synthesis of transparent high refractive index sulfur-containing polymers,” *Sci. Adv.*, vol. 6, no. 28, p. eabb5320, 2020.
- [106] C. Poddar, S. Ningshen, and J. Jayaraj, “Corrosion assessment of Ni₆₀Nb₃₀Ta₁₀ metallic glass and its partially crystallized alloy in concentrated nitric acid environment,” *J. Alloys Compd.*, vol. 813,

- p. 152172, 2020.
- [107] G. Scheen *et al.*, “Post-process porous silicon for 5G applications,” *Solid. State. Electron.*, vol. 168, p. 107719, 2020.
- [108] X. F. Gao, “In-situ exfoliation of porous carbon nitride nanosheets for enhanced hydrogen evolution,” *Nano Energy*, vol. 59, pp. 598–609, 2019.
- [109] Jin, Long Xiao, Xiao Deng, Weili Nashalian, Ardo He, Daren Raveendran, Vidhur Yan, Cheng, “Manipulating relative permittivity for high-performance wearable triboelectric nanogenerators,” *Nano Lett.*, vol. 20, no. 9, pp. 6404–6411, 2020.
- [110] S.T. Fleischmann, “Continuous transition from double-layer to Faradaic charge storage in confined electrolytes,” *Nat. Energy*, vol. 7, no. 3, pp. 222–228, 2022.
- [111] B. C. Reddy, “Synthesis and characterization of multi functional nickel ferrite nano-particles for X-ray/gamma radiation shielding, display and antimicrobial applications,” *J. Phys. Chem. Solids*, vol. 159, p. 110260, 2021.
- [112] H. Wu, T. Kudo, T. Takahashi, T. Ito, and S.-Y. Kim, “Impregnation of covalent organic framework into porous silica support for the recovery of palladium ions from simulated high-level liquid waste,” *J. Radioanal. Nucl. Chem.*, vol. 330, no. 3, pp. 1065–1074, 2021.
- Jeong, Moonkyoung Jung, Yuna Yoon, Junyong Kang, Jinyoung [113] Lee, Seo Hyeon Back, Woojin Kim, Hyoyeon Sailor, Michael J Kim, Dokyoung Park, Ji-Ho, “Porous Silicon-Based Nanomedicine for Simultaneous Management of Joint Inflammation and Bone

References

Erosion in Rheumatoid Arthritis,” *ACS Nano*, 2022.

[114] T. Zhong, W. Yu, C. Shen, and X. Wu, “Research on preparation and characterisation of high-purity silica sands by purification of quartz vein ore from dabie mountain,” *Silicon*, vol. 14, no. 9, pp. 4723–4729, 2022.

الخلاصة

دُرس السيليكون المسامي من خلال الخصائص الفيزيائية والكيميائية والتركيبية

تمت دراسة و مقارنة نتائج الحوامض المستخدمة (حامض الهيدروفلوريك + الايثانول ، حامض النترريك + حامض الهيدروفلوريك ، حامض النترريك + الملح NaCl) من خلال دراسة الخصائص المورفولوجيا والتركيبية لطبقات السيليكون المسامي باستعمال المجهر الالكتروني الماسح (SEM) و حيود الاشعة السينية (XRD) و الطريقة الوزنية .

من خلال صور المجهر الالكتروني لعينات السيليكون المسامي فقد تبين ان هناك اشكال مختلفة للسيليكون المسامي اذ يختلف الشكل باختلاف زمن التفاعل و تأثير الحامض المستخدم.

بينت النتائج ان قطر المسام وسمك طبقة السيليكون المسامي تزداد باستعمال حامض النترريك مع HF اكثر من HF مع الايثانول.

وان المسامية المقاسة باستعمال الطرائق الوزنية تختلف باختلاف الحوامض المستخدمة لإنتاج السيليكون المسامي وقد ظهرت بقيم عالية في حامض النترريك اكثر من الايثانول مع HF

درست الخصائص البصرية والكهربائية لعينات الحوامض و تبين ان هذه الخصائص تتأثر بسمك الطبقة فزيادة سمك الطبقة تقل النفاذية النسبية ومعامل الانكسار وبالعكس

السعة الكهربائية تتأثر بالمسامية وسمك الطبقة اذا تقل كلما كانت الطبقة المسامية اكبر بسبب كمية الشحنات والايونات الموجودة اما عندما تكون الطبقة المسامية صغيرة فتقل بسبب وجود الهواء

السعة الكهربائية للسيليكون النانوي المعالج في محلول HF مع الايثانول يكون اعلى بكثير من HF مع HNO₃

اختلاف قياس الابعاد النانوية للمسام خلال الاوقات المختلفة لحامض الايثانول + HF منتظم اكثر وصفاتها النانوية تكون اوضح لان كلما كان المسام اصغر كلما كان الصفات النانوية اوضح

كل الحالات لها تطبيق معين فيتم استخدام الحامض حسب التطبيق المطلوب.

بينت النتائج ان السيليكون يتفاعل مع حامض النترريك لإنتاج الاكسيد الذي يذوب في حامض الهيدروفلوريك و هكذا فان التفاعل مع حامض النيتريك بوجود HF اعطى افضل واجود سيليكون مسامي.

بشكل عام ، فإن خصائص إنتاج السيليكون المسامي من تفاعل السيليكون مع الأحماض يؤدي إلى تحسين هذه الخصائص المسامية في ضوء أي تطبيق للسيليكون البلوري النانوي



جمهورية العراق

وزارة التعليم العالي والبحث العلمي

جامعة كربلاء

كلية التربية للعلوم الصرفة

قسم الكيمياء

مقارنة بين ثلاث محاليل لإنتاج السيليكون المسامي

رسالة مقدمة الى

مجلس كلية التربية للعلوم الصرفة - جامعة كربلاء

وهي جزء من متطلبات نيل درجة الماجستير في الكيمياء

تقدمت بها

فرقان صالح مهدي

(بكالوريوس 2019)

بإشراف

أ.د حميدة عيدان سلمان

أ.م.د احمد خير الله شهيد الكاظمي